JOURNAL *of the*
BOSTON SOCIETY OF CIVIL ENGINEERS

1848
BOSTON
SOCIETY
OF CIVIL
ENGINEERS

121 YEARS
1848-1969

JANUARY — 1969

VOLUME 56 NUMBER 1

JOURNAL OF THE
BOSTON SOCIETY
OF
CIVIL ENGINEERS

Volume 56 JANUARY 1969 Number 1

CONTENTS

Journal of Boston Society of Civil Engineers is indexed regularly by Engineering Index, Inc.

Second-Class postage paid at Boston, Massachusetts

Published four times a year, January, April, July and October, by the Society
47 Winter Street, Boston, Massachusetts 02108

Subscription Price $7.00 a Year (4 Copies)
$1.75 a Copy
All orders must be accompanied by check

JOURNAL OF THE
BOSTON SOCIETY OF CIVIL ENGINEERS

Volume 56 JANUARY 1969 Number 1

HYDRAULICS OF MIXING TANKS

by THOMAS R. CAMP*, *Past President*

(1969 John R. Freeman Memorial Lecture, presented before the Boston Society of Civil Engineers and the Hydraulics Section on January 22, 1969.)

Introduction

Mixing is widely used in the chemical and pharmaceutical industries to disperse additives throughout liquids or to homogenize two or more liquids. A measure of effectiveness of such mixing is the uniformity of dispersion. A frequent purpose of mixing is to promote chemical or biochemical reactions.

In the treatment of water or wastewater in continuous-flow plants, mixing is used for all of the above purposes, but one of the most important functions is the flocculation of impurities with coagulants so that they may be removed by settling or filtration. It has become common practice to provide a rapid initial or flash mix for dispersion of the coagulants or other chemicals throughout the influent followed by two or more larger chambers in series where floc growth takes place. Mixing propellers or flat blade turbines are usually used in the flash mix, and rotor reels in the floc chambers.

In 1943, the author and P. C. Stein[1] demonstrated that the time rate of flocculation (i.e., agglomeration into larger particles) is directly proportional to the velocity gradient (i.e., space rate of change of velocity) at a point. The velocity gradients vary considerably throughout a mixing tank, but under steady conditions of mixing, a mean velocity gradient related to the energy dissipation per unit of tank volume may be used. The relation between the velocity gradient and the energy dissipated per unit volume was derived by the authors from the original analysis by Sir G. G. Stokes[2] in 1845.

All of the energy dissipated in a moving or stirred liquid is by shear within the liquid, and heat is evolved to increase the temperature of the liquid. The instantaneous shearing stress at a point is

$$\tau = \mu \frac{dv}{ds} \tag{1}$$

* Partner Emeritus Camp, Dresser & McKee, Consulting Engineers, Boston, Massachusetts

where $\frac{dv}{ds}$ is the *absolute velocity gradient* at the point and the proportionality constant μ is the *absolute viscosity* of the liquid. The *root-mean-square velocity gradient* for a container is

$$G = \sqrt{\frac{W}{\mu}} \tag{2}$$

where W is the energy dissipated per unit volume, called the *dissipation function* by Stokes. The author[3] has recently demonstrated by extensive experiments with hydrous ferric oxide floc that the floc size and volume concentration may be varied over a wide range by changes in G. The principal constituent of floc (less than 85 to more than 99%) is loosely bound water, the amount of which is controlled by G.

The value of W depends upon the geometry of the rotors, stators and container, and upon the speed of the rotors. Accurate values of W can be determined only by measurement of the torque input to the liquid at various speeds and liquid temperatures. The value of W in terms of the speed and measured torque is

$$W = \frac{2\pi ST}{V} \tag{3}$$

where S is the measured rotor speed in rps, T is the measured torque input and V is the liquid volume.

The calibration curves for G shown in Fig. 1 were computed by means of Eqs. (2) and (3) from numerous measurements of torque input at the water temperatures shown. These curves are for 2 liters of water in a 2-liter beaker, both with and without stators. All dimensions are shown on the figure. The torque measurements were made by supporting the beaker on a platform suspended on a piano wire, and by direct connection of the rotor shaft to a motor mounted on a thrust ball bearing ring. Torque measurements may be made for a large mixing tank by inserting a torque meter in the rotor shaft above the water surface for vertical shafts or in a dry well for horizontal shafts, provided the tank is designed to permit the insertion. Accurate torque meters are commercially available for this purpose. Since the purpose of calibration of a mixing tank is to determine the power dissipated *in the liquid*, torque measurements at each speed must be made with the tank both full and empty. The difference is the net torque for the liquid.

The computed points on Fig. 1 indicate some errors in measurements of torque or speed. The curves were adjusted for a smooth fit of the plotted points. For fully turbulent drag, the ordinates for a particular speed should be inversely proportional to the square roots of the viscosities as required

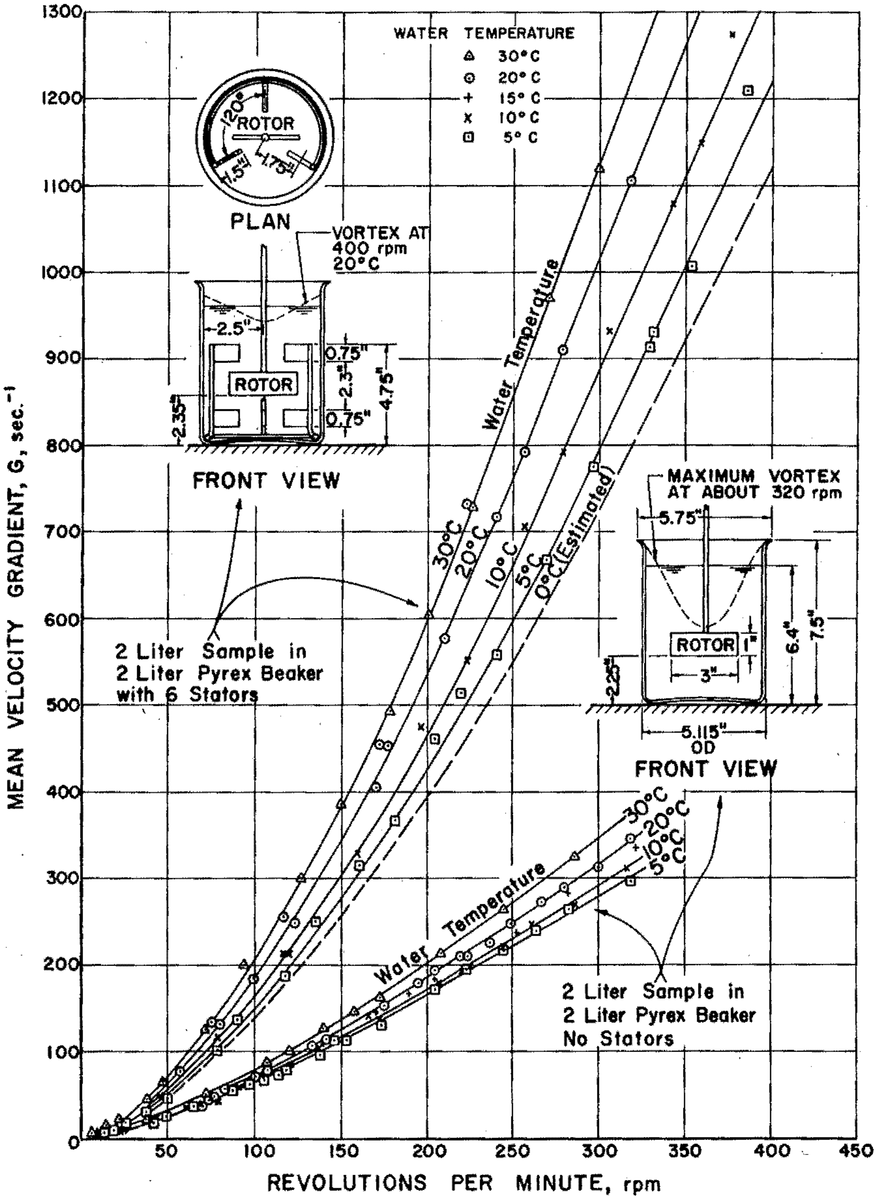

Fig. 1 — Velocity gradient calibration curves for water.

by Eqs. (2) and (4). This relationship is met for the case with stators at all speeds above about 20 rpm, as later shown by Fig. 3, but for the case without stators, the drag is not fully turbulent until the speed is greater than 300 rpm. For fully streamline drag at a particular speed, there is only one value of G for all viscosities as required by Eqs. (2) and (5). This condition is met at speeds less than 5 rpm for the case with stators, and 10 rpm for the case without stators.

The speed without stators was limited to about 320 rpm, which produced a vortex extending down almost to the top of the rotor blade, as shown in Fig. 1. The effect of the stators is to reduce the vortex in all cases and greatly increase the values of G at all speeds. Fig. 1 shows an increase of G by the stators of more than 3-fold at the higher speeds, which corresponds with about a 10-fold increase in the power dissipated. It is obvious from Fig. 1 that mixing tanks and equipment cannot be designed accurately solely on the basis of rotor drag, as assumed by the author in an earlier paper[4] (1955), and that stator and wall drag must also be included.

Gross Drag Coefficients

In order to design a mixing chamber to produce a desired range of values for G or W within a desired range of speeds, it is convenient to express the dissipation function W in terms of the drag on the rotors, stators and walls. Extensive velocity measurements in vertical cylindrical vessels with turbine blades on vertical shafts by Nagata *et al*, Aiba and others, as reported by Gray[5], indicate that the radial and vertical velocity components are small as compared to the tangential velocity components, and that the tangential velocity is directly proportional to the radial distance out from the center of the shaft almost to the tip of the turbine blades. Beyond the tip of the blades, the tangential velocity decreases in some cases and is approximately constant in others. The radial distribution of the tangential velocity is about the same throughout the depth. The tangential velocity of the liquid is reduced with stators.

To simplify the theoretical development, the author has assumed that all of the energy dissipation is associated with the tangential velocity components of the liquid, and that this velocity is directly proportional to the radial distance out from the center of the shaft to a maximum at the tips of the rotor paddles and is constant beyond the paddle tips. The assumed distribution of tangential velocity is shown in Fig. 2. The velocity, v, of the liquid at any radial distance r less than r_r at the tip of the rotor is $2\pi rkS$, and beyond the rotor tip is $2\pi r_r kS$; where kS is the speed of the water in

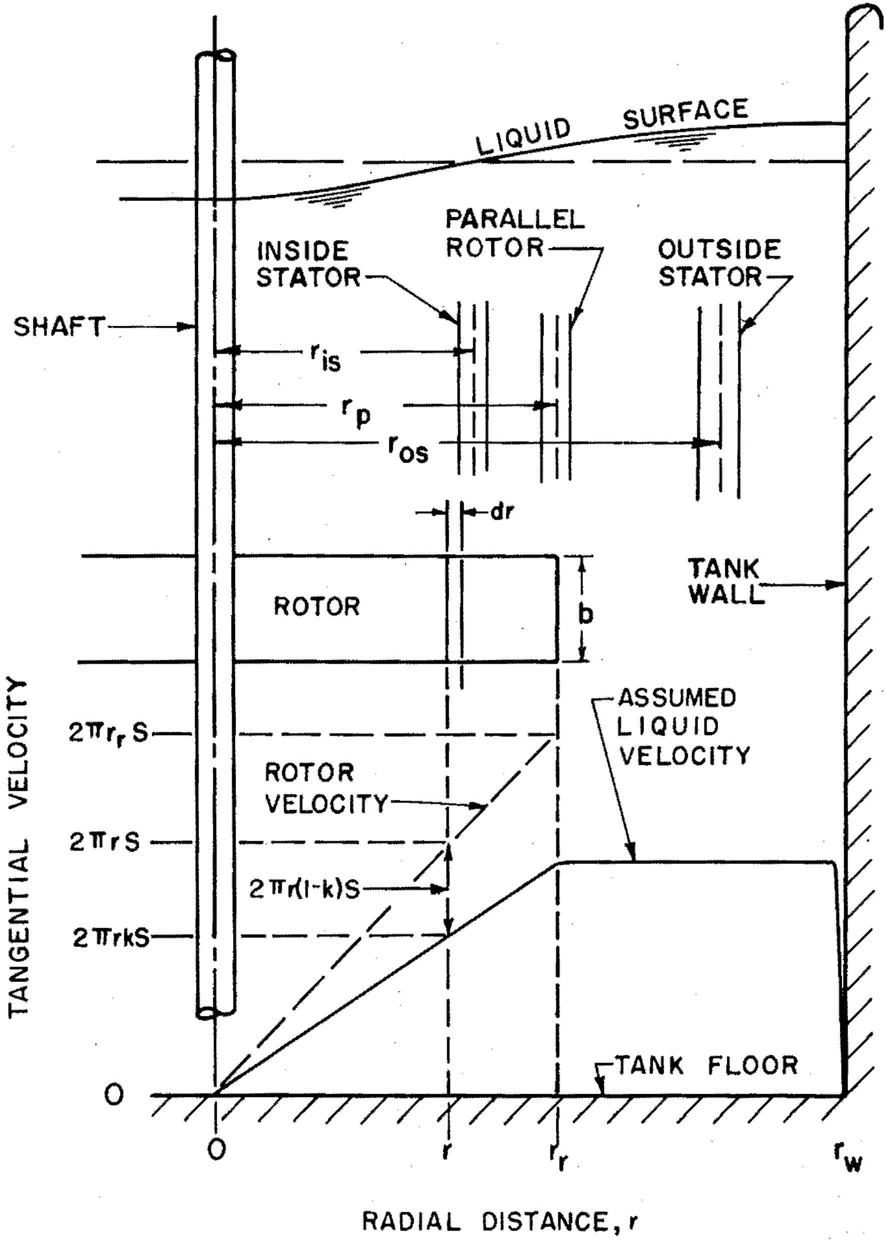

Fig. 2 — Assumed distribution of Tangential Liquid Velocity in mixing tank.

rps. Since the energy dissipated in turbulent drag is proportional to $\rho \frac{v^3}{2}$, the value of the dissipation function W in terms of turbulent drag on rotors, stators and walls is:

$$W = 124\rho a C_t S^3 \tag{4}$$

where 124 is $\frac{(2\pi)^3}{2}$, ρ is the mass density of the liquid; a is the projected area of the rotor blades, and C_t is a dimensionless *turbulent gross drag coefficient* determined by the geometry of the system. The term a is introduced solely for the purpose of making C_t dimensionless.

For any speed S, C_t may be computed by means of Eqs. (3) and (4) from the corresponding measured value of the torque T, or by means of Eq. (2) from the corresponding value of G on one of the calibration curves for velocity gradient. The better procedure is to use a calibration curve for G for a selected temperature because these curves are already adjusted to reduce experimental error. Fig. 3 is a log-log plot of the gross drag coefficients, C_t against rpm computed in this manner for the 2-liter beaker with water at 30°C. For lower water temperatures, the curves will be approximately in the same position for fully turbulent drag and will be higher in proportion to the viscosity for fully streamline drag.

Fig. 3 is enlightening in several respects. First, it is remarkably similar to well known plots of friction factor or drag coefficient against Reynolds number. Second, it clearly shows the existence of a streamline region, at speeds below 5 rpm, with stators, and below 10 rpm without stators, for the particular example. Third, the drag in the example is fully turbulent with stators at about 30 rpm but, without stators, is not fully turbulent at speeds up to about 300 rpm. Since the effectiveness of mixing depends upon the degree of turbulence, it is evident that the stators in the 2-liter beaker make an important contribution. For example, full turbulence is present with the stators at 30 rpm and a G of about 30, whereas, without stators, full turbulence is not present at 300 rpm even though G is about 350.

The curves for C_t, illustrated on Fig. 3, are based on fully turbulent drag which is assumed to be proportional to v^2. This proportionality does not hold except where the curves are nearly horizontal. In the streamline region, the drag is proportional to v and C_t becomes inversely proportional to the Reynolds number. Since the speed of the rotors is the only changeable factor in the Reynolds number for a particular mixing tank and water temperature, the curves for C_t in the streamline region slope downwards on the log-log plot at 45°. It becomes apparent that the dissipation function W

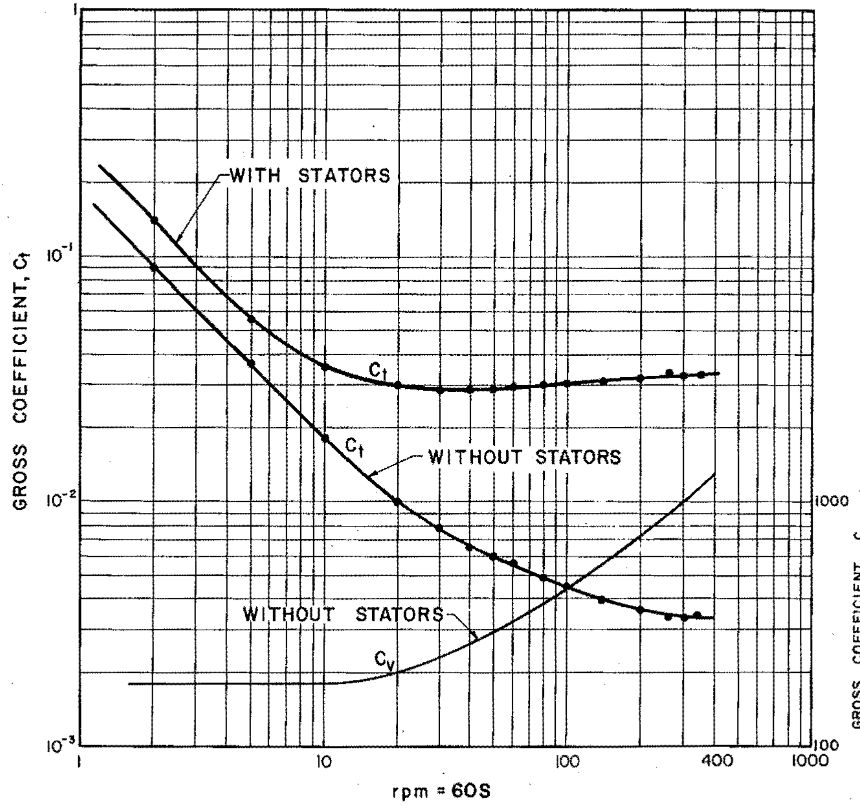

Fig. 3 — Gross drag coefficients for 2-Liter Beaker with water at 30°C.

may also be expressed in terms of the viscous drag, where energy is dissipated in proportion to μv^2, as follows:

$$W = 4.92 \mu C_V S^2 \tag{5}$$

where 4.92 is $\frac{(2\pi)^2}{8}$ and C_V is a dimensionless *viscous gross drag coefficient* determined by the geometry of the system. Fig. 3 shows a curve for values of C_V for the 2-liter beaker without stators, which illustrates that the curve is horizontal in the streamline region and slopes upward at 45° in the fully turbulent region.

Plots of C_V are not necessary because the value of C_V may be computed for any rotor speed from the corresponding value of C_t taken from the curve. The value of C_V in terms of C_t may be obtained by equating the values of W in Eqs. (4) and (5) as follows:

$$C_V = \frac{25.1}{\nu} a C_t S \tag{6}$$

where 25.1 is 8π and υ is the kinematic viscosity of the liquid or $\frac{\mu}{\rho}$.

The value of the turbulent gross drag coefficient, C_t in terms of the drag on the rotors, stators and walls is

$$C_t = \frac{C_D}{Va}\left[(1-k)^3 A + k^3 (B + \frac{f}{C_D} C)\right] \tag{7}$$

where C_D is the conventional turbulent drag coefficient applied to the system of rotors and stators, f is the Weisbach-Darcy wall friction factor, and A, B and C are the dimensional turbulent work parameters for the rotors, stators and walls, respectively.

The value of the viscous gross drag coefficient, C_V, in terms of the drag on the rotors, stators and wall is

$$C_V = \frac{C_D'}{V^2}\left[(1-k)^2 A' + k^2 (B' + \frac{f'}{C_D'} C')\right] \tag{8}$$

where C_D' is C_D times the Reynolds number, f′ is f times the Reynolds number, and A′, B′ and C′ are the dimensional viscous work parameters for the rotors, stators and walls, respectively.

The dimensional work parameters are derived hereinafter in the Appendix for various types of rotors and stators in terms of the areas and radii. The dimensions of the turbulent work parameters are $(\text{length})^5$, and the dimensions of the viscous work parameters are $(\text{length})^6$.

Eq. (7) for C_t is applicable only where turbulence is fully developed and does not change appreciably with change in speed. Eq. (8) for C_V is applicable only where flow is streamline and C_V does not change appreciably with change in speed. It is proposed to use these equations in design to estimate the position of the two tangents to the C_t curve on log-log paper.

Evaluation of Coefficients

In order to use the gross drag coefficients for design, torque measurements were made on existing tanks to evaluate friction factors and drag coefficients. The factor k may be estimated by equating the moment of the drag on the rotors to the moment of the drag on the stators and walls, each of which is equal to the torque. The drag and friction coefficients may be estimated by assuming that at the same speed they have the same values without the stators in place as with the stators. This requires evaluation of C_t for both cases, as illustrated on Fig. 3.

Drag Moments

The moments of the turbulent drag are proportional to $\rho \frac{v^2}{2} r$, as follows:

Rotors $$M_r = 19.7\,\rho\, C_D (1-k)^2 A_m S^2 \qquad (9)$$

Stators $$M_s = 19.7\,\rho\, C_D k^2 B_m S^2 \qquad (10)$$

Walls $$M_w = 19.7\,\rho\, C_D k^2 \frac{f}{C_D} C_m S^2 \qquad (11)$$

where 19.7 is $\frac{(2\pi)^2}{2}$ and A_m, B_m and C_m are the dimensional moment parameters for turbulent drag on rotors, stators and walls, respectively.

The moments of the viscous drag are proportional to $\mu v r$, as follows:

Rotors $$M'_r = 0.785\mu \frac{C'_D}{V} (1-k) A'_m S \qquad (12)$$

Stators $$M'_s = 0.785\mu \frac{C'_D}{V} k\, B'_m S \qquad (13)$$

Walls $$M'_w = 0.785\mu \frac{C'_D}{V} k \frac{f'}{C'_D} C'_m S \qquad (14)$$

where 0.785 is $\frac{2\pi}{8}$ and A'_m, B'_m and C'_m are the dimensional moment parameters for viscous drag on rotors, stators and walls, respectively.

The dimensional moment parameters are derived hereinafter in the Appendix for various types of rotors and stators in terms of the areas and radii. The dimensions of the turbulent moment parameters are $(\text{length})^5$ and of the viscous moment parameters are $(\text{length})^6$.

Turbulent Coefficients

Equating the moments of turbulent drag,

$$k^2 (B_m + \frac{f}{C_D} C_m) = (1-k)^2 A_m \tag{15}$$

from which,

$$k = \frac{1}{1 + \sqrt{\dfrac{B_m + f/C_D C_m}{A_m}}} \tag{16}$$

and

$$\frac{f}{C_D} = \frac{(1-k)^2}{k^2} \frac{A_m}{C_m} - \frac{B_m}{C_m} \tag{17}$$

Since $\frac{f}{C_D} > 0$

$$\frac{(1-k)^2}{k^2} A_m > B_m \tag{18}$$

and

$$k < \frac{1}{1 + \sqrt{\dfrac{B_m}{A_m}}} \tag{19}$$

From (19), for the case without stators, B_m is zero and k is less than 1.0. For the case with stators, k_s is less than a fraction of 1.0. For example, for the 2-liter beaker with stators where B_m, A_m and C_m are 10.67×10^{-5}, 1.017×10^{-5} and 67.5×10^{-5} ft^5,

$$k_s < \frac{1}{1 + \sqrt{\dfrac{10.67 \times 10^{-5}}{1.017 \times 10^{-5}}}} < 0.236$$

If from Eq. (17) the values of $\frac{f}{C_D}$ for the cases with and without stators are equated, the following results:

$$\frac{(1-k_s)^2}{k_s^2} - \frac{(1-k)^2}{k^2} = \frac{B_m}{A_m} \tag{20}$$

where k is for the case without stators and k_s is for the case with stators.

If the moment of the drag on the rotors of Eq. (9) is set equal to the torque of Eq. (3), the following results:

$$W = 124 \rho a \frac{C_D}{Va} (1-k)^2 A_m S^3 \tag{21}$$

in which, by comparison with Eq. (4),

$$C_t = \frac{C_D}{Va}(1-k)^2 A_m \tag{7a}$$

It is evident from Eq. (7a) that for fully turbulent drag,

$$\frac{(1-k_s)^2}{(1-k)^2} \doteq \frac{C_t \text{ with stators}}{C_t \text{ without stators}} \tag{22}$$

With known values of C_t for the two cases, the values of all coefficients can be determined by trial-and-error solutions of Eqs. (22), (19), (20), (17), (16), and (7a). For example, for the 2-liter beaker at 300 rpm, C_t is 3.4×10^{-2} with stators and 0.33×10^{-3} without stators. From (22),

$$\frac{(1-k_s)^2}{(1-k)^2} = \frac{3.4}{0.33} = 10.3 \text{ and } \frac{1-k_s}{1-k} = 3.21$$

From (19), k_s is less than 0.236, and by successive trials by (20) k_s is equal to 0.235, from which $1-k_s$ is 0.765. From the above ratio, 1-k is $\frac{0.765}{3.21}$ or 0.238, from which k is 0.762. Check by Eq. (20)

$$\left(\frac{0.765}{0.235}\right)^2 - \left(\frac{0.238}{0.762}\right)^2 = 10.585 - 0.098 = 10.49 = \frac{10.67}{1.017}$$

From 17,

$$\frac{f}{C_D} = 0.098\,\frac{1.017}{67.5} = 0.00147$$

Check by (16)

$$k_s = \frac{1}{1+\sqrt{\dfrac{10.67 + 0.00147 \times 67.5}{1.017}}} = 0.235$$

and

$$k = \frac{1}{1+\sqrt{\dfrac{0.00147 \times 67.5}{1.017}}} = 0.762$$

For V of 0.0706 ft³, from Eq. (7a),

$$C_D = \frac{C_t Va}{(1-k_s)^2 A_m} = \frac{3.4 \times 10^{-2} \times 0.706 \times 10^{-1} \times 2.08 \times 10^{-2}}{0.765^2 \times 1.017 \times 10^{-5}} = 8.4$$

and $f = 0.00147 \times 8.4 = 0.0123$

Viscous Coefficients

Equating the moments of the viscous drag,

$$k(B_m' + \frac{f'}{C_D'} C_m') = (1 - k) A_m' \qquad (23)$$

From which
$$k = \frac{1}{1 + \dfrac{B_m' + f'/C_D' C_m'}{A_m'}} \qquad (24)$$

and
$$\frac{f'}{C_D'} = \frac{1-k}{k} \frac{A_m'}{C_m'} - \frac{B_m'}{C_m'} \qquad (25)$$

Since $\dfrac{f'}{C_D'} > 0$
$$\frac{1-k}{k} A_m' > B_m' \qquad (26)$$

and
$$k < \frac{1}{1 + \dfrac{B_m'}{A_m'}} \qquad (27)$$

From (27), for the case without stators, B_m' is zero and k is less than 1.0. For the case with stators, k is less than some fraction of 1.0. For example, for the 2-liter beaker with stators, where B_m', A_m' and C_m' are 40.0×10^{-6}, 2.26×10^{-6} and 4.49×10^{-3} ft^6.

$$k_s < \frac{1}{1 + \dfrac{40.0 \times 10^{-6}}{2.26 \times 10^{-6}}} < 0.0535$$

If from (25), the values of $\dfrac{f'}{C_D'}$ for the cases with and without stators are equated, the following results:

$$\frac{1-k_s}{k_s} - \frac{1-k}{k} = \frac{B_m'}{A_m'} \qquad (28)$$

where k is for the case without stators and k_s is for the case with stators.

If the moment of the drag on the rotors of Eq. (12) is set equal to the torque of Eq. (3), the following results:

$$W = 4.92\mu \frac{C_D'}{V^2} (1 - k) A_m' S^2 \qquad (29)$$

in which, by comparison with Eq. (5),

$$C_V = \frac{C_D'}{V^2} (1 - k) A_m' \tag{8a}$$

It is evident from Eq. (8a) and Eq. (6) that for streamline drag at the same rpm,

$$\frac{1 - k_s}{1 - k} = \frac{C_V \text{ with stators}}{C_V \text{ without stators}} = \frac{C_t \text{ with stators}}{C_t \text{ without stators}} \tag{30}$$

With known values of C_t for the two cases, all coefficients can be evaluated by trial-and-error solutions of Eqs. (30), (27), (28), (25), (24), and (8a). For example, for the 2-liter beaker at 3 rpm, C_t is 9.32×10^{-2} with stators and 5.96×10^{-2} without stators. From (30),

$$\frac{1 - k_s}{1 - k} = \frac{9.32}{5.96} = 1.56$$

From (27), k_s is less than 0.535, and by successive trials by (28) k_s is equal to 0.049 from which $1 - k_s$ is 0.951. From the above ratio, 1-k is 0.609, from which k is 0.391. Check by (28),

$$\frac{0.951}{0.049} - \frac{0.609}{0.391} = 19.28 - 1.56 = 17.72 \quad \frac{B_m'}{A_m'} = \frac{40}{2.26} = 17.7$$

From (25), $\frac{f'}{C_D'} = 1.56 \frac{2.26}{4490} = 0.785 \times 10^{-3}$ Check by (24),

$$k_s = \frac{1}{1 + \frac{40 \times 10^{-6} + 0.785 \times 4.49 \times 10^{-6}}{2.26 \times 10^{-6}}} = 0.049$$

and

$$k = \frac{1}{1 + \frac{0.785 \times 4.49 \times 10^{-6}}{2.26 \times 10^{-6}}} = 0.392$$

For water at 30°C, $\upsilon = 0.86 \times 10^{-5}$ ft²/sec, and from Eq. (6) for 3 rpm

$$C_V = \frac{25.1}{0.86 \times 10^{-5}} \times 2.08 \times 10^{-2} \times 5.96 \times 10^{-2} \times \frac{3}{60} = 181 \text{ without stators}$$

For V of 0.0706 ft³, from Eq. (8a),

$$C_D' = \frac{C_V V^2}{(1-k)A_m'} = \frac{181 \times 0.706^2 \times 10^{-2}}{0.609 \times 2.26 \times 10^{-6}} = 6.57 \times 10^5$$

and $$f' = 0.785 \times 10^{-3} \times 6.57 \times 10^5 = 516$$

Principle of Least Work

The author believes that the Principle of Least Work is a natural law universally applicable. This principle holds that nature is lazy and follows the path of least resistance with minimum work in all of its actions. It has been used in analyses of indeterminate structures where it is assumed that under an applied load the stresses will be distributed so that the total work done in deformation is a minimum. Since this principle has been badly neglected in fluid dynamics, the author has studied it as another means for the evaluation of k.

If the partial derivative with respect to k of the work W, and therefore of C_t and C_V in Eqs. (7) and (8), is set to equal to zero, equations similar to (15) and (23) result. The dimensional parameters, however, are the work parameters instead of the moment parameters. The work parameters are the same as the moment parameters for the rotors and inside stators where the same value of r is used for the moment arm and tangential velocity, as shown on Fig. 2. The parameters differ, however, for outside stators and the walls, because the velocity is determined by r_r and the moment arms are r_{os} and r_w, respectively.

The value of k determined by the least work method does correspond with the minimum value of W, but the method is incorrect because the requirement that the input moment must equal the resisting moment is not met for the assumed distribution of the velocity. Nevertheless, solutions by least work are approximately correct. For example, for the 2-liter beaker, the error in C_D is +3.6% and in C_D' is +0.3%, and the errors in k_s are +6.0% for turbulent drag and +14% for viscous drag. It is evident that the Principle of Least Work does apply to this case, provided the drag moments are also equal.

Dimensional Effects

In order to study the effects on drag and wall friction coefficients of tank shape and paddle arrangements, extensive exploratory torque measurements were made with water in the units of a small pilot plant consisting of a rapid mix tank 4.4 in. sq. by 3 ft. deep, followed by 3 tanks each 1.0 ft. sq. by 3 ft. deep with vertical shafts. The rapid mix tank was designed to produce G-values of about 30 to 1000 with water up to 30°C and fully turbulent mixing. The first 1.0 ft. sq. tank was designed to produce, with fully turbulent mixing, G-values of about 30 to 750, and the second and third tanks, G-values of about 10 to 100. One of the larger tanks was filled to a depth of 1 ft. of water to study the effects of a cubic-shaped tank, and the paddles were designed to produce G-values of about 30 to 500 with full turbulence.

The results of the torque measurements are shown in Table 1. Column 1 shows the data for the 2-liter beaker, column 2 for the 4.4 in. sq. rapid mix tank, column 3 for the first 1 ft. sq. by 3 ft. deep tank, column 4 for the second and third 1 ft. sq. by 3 ft. deep tank, and column 5 for the 1 ft. sq. by 1 ft. deep tank.

The first measurements, made with rotor blades vertical, resulted in large vortices at high speeds. The vortices were eliminated by pitching the blades 45° with the vertical, and placing the top rotor assemblies to pump upward. Hoerner[6] has published the results of experiments which show that the turbulent drag coefficient is approximately constant with plates tilted against the direction of flow from 90° to 45°. It is therefore permissible to use the projected plate area for pitched blades, provided the pitch is not less than 45° against the direction of flow. Experiments conducted with the 4.4 in. sq. tank with rotor blades vertical and tilted 45°, but without stators, showed that the turbulent torque with the pitched blades was about 75.5% of the torque with blades at 90° with the direction of flow. Since the projected area was reduced to 70.7% of the area of the vertical blades, the difference indicates an increase of about 7% in the value of $(1\text{-}k)^2$ in Eq. (9).

The small tank was equipped with 4 rotors 3 inches in diameter at depths of 12, 19, 26 and 33 inches below the water surface. Each rotor has 6 radial blades attached to its hub at 60° intervals and pitched 45° with the vertical. Each blade is 1 in. wide by 1-1/16 in. long. The value of a is 0.125 sq. ft. The top and third rotors pump upwards, and the other two downwards. The stators consist of 12 blades, each 2-1/2 in. high by 1-1/2 in. wide, placed in radial vertical planes through the corners with the inside edges 0.9 in. from the center of the shaft. Three blades are in each corner spaced vertically between rotors.

The first large tank has 4 rotors 8 in. in diameter at depths of 3-3/8, 16-1/4, 19-3/4 and 32-5/8 in. below the water surface. Each rotor has 6 radial blades attached to its hub at 60° intervals and pitched 45° with the vertical. Each blade is 1 in. wide by 3-5/8 in. long. The rotor area, a, is

TABLE I. EFFECTS OF DIMENSIONS ON COEFFICIENTS, WATER AT 30° C.

CONTAINER	(1) 5" DIA. 6.4" DEEP	(2) 4.4" SQ. 3' DEEP	(3) 1.0' SQ. 3' DEEP	(4) 1.0' SQ. 3' DEEP	(5) 1.0' SQ. 1' DEEP
TURBULENT					
A_m ($ft.^5 \times 10^4$)	0.1017	0.855	45.21	5.16	22.3
B_m ($ft.^5 \times 10^4$)	1.067	6.102	324.4	223.3	147.0
C_m ($ft.^5 \times 10^4$)	6.75	32.4	1810.0	1018.0	695.0
C_{t_s}/C_t	10.3	1.44	1.70	1.55	1.56
k_s	0.235	0.2397	0.2498	0.1252	0.2514
k	0.762	0.3689	0.4240	0.2976	0.3989
f	0.0123	0.1365	0.0804	0.0472	0.1072
C_D	8.4	1.76	1.735	1.632	1.469
STREAMLINE					
A_m' ($ft.^6 \times 10^4$)	0.0226	1.12	76.5	3.18	18.56
B_m' ($ft.^6 \times 10^4$)	0.400	8.75	516.2	693.2	86.8
C_m' ($ft.^6 \times 10^4$)	44.90	1150.0	70500.0	52800.0	10420.0
C_{t_s}/C_t	1.56	1.13	1.34	1.44	1.38
k_s	0.049	0.0941	0.1025	0.0045	0.1393
k	0.391	0.3554	0.3329	0.3094	0.3996
f'	516.0	918.0	2170.0	511.0	1395.0
$C_D' \times 10^{-5}$	6.57	5.18	9.96	37.9	5.23

0.433 sq. ft. The third rotor from the top pumps down and the other three upwards. There are 8 stators, each 6 in. high by 3 in. wide, placed in radial vertical planes through the corners with the inside edges 2.5 in. from the center of the shaft. Two blades are in each corner spaced vertically between the two top and two bottom rotors, respectively.

The second large tank (and the third) has 3 rotors 6 in. in diameter at depths of 3-3/8, 18 and 32-5/8 in. below the water surface. Each rotor has 3 radial blades attached to its hub at 120° intervals and pitched 45° with the vertical. Each blade is 1 in. wide by 2-5/8 in. long. The rotor area, a, is 0.116 sq. ft. The middle rotor pumps down and the other two upwards. The stators are identical with those in the first large tank.

The cubic tank has 2 rotors 8 in. in diameter at depths of 4 and 8 in. below the water surface. Each rotor has 6 radial blades attached to its hub at 60° intervals and pitched 45° with the vertical. Each blade is 1 in. wide by 3-5/8 in. long. The projected rotor area, a, is 0.2135 sq. ft. The top rotor pumps upwards and the bottom rotor downwards. There are 12 stators, each 1-1/2 in. high by 3 in. wide, placed in radial vertical planes through the corners with the inside edges 3 in. from the center of the shaft. Three blades are in each corner, 1.9, 6 and 10.1 in. below the water surface.

Table 1 shows very significant differences between cylindrical and square tanks in the region of turbulent drag. The drag coefficient C_D is much greater and the wall friction factor f much less for the cylindrical tank than for the square tanks, which results in a much higher value for $C_{\uparrow}/C_{\uparrow_s}$ for the cylindrical tank. Figs. 4 to 7 show that turbulent drag can be obtained over a much wider speed range in square tanks both with and without stators than is the case with cylindrical tanks.

Design of Tanks

The size and dimensions of a mixing tank are usually determined by the volume desired or retention period for continuous flow units. The design procedure thereafter is best illustrated by an example: a rapid-mix tank 10 ft. by 12 ft. in plan with a 13 ft. water depth constructed in an expansion of the Billerica (Massachusetts) water treatment plant. It is proposed to dissipate 10 hp, or 3.53 ft. lb. per sec per cf for a volume of 1560 cf. The maximum value of G for this value of W will range from 311 sec^{-1} at 2°C. to 471 at 30°C.

Two six-blade rotors, 6 ft. in diameter and 5 ft. on centers, are mounted on a vertical shaft; the top rotor to pump upward, and the bottom downward. Each blade is 8 in. wide by 2.62 ft. long and pitched 45° with the vertical. The projected area of the rotor blades, a, is 14.8 sq. ft. There

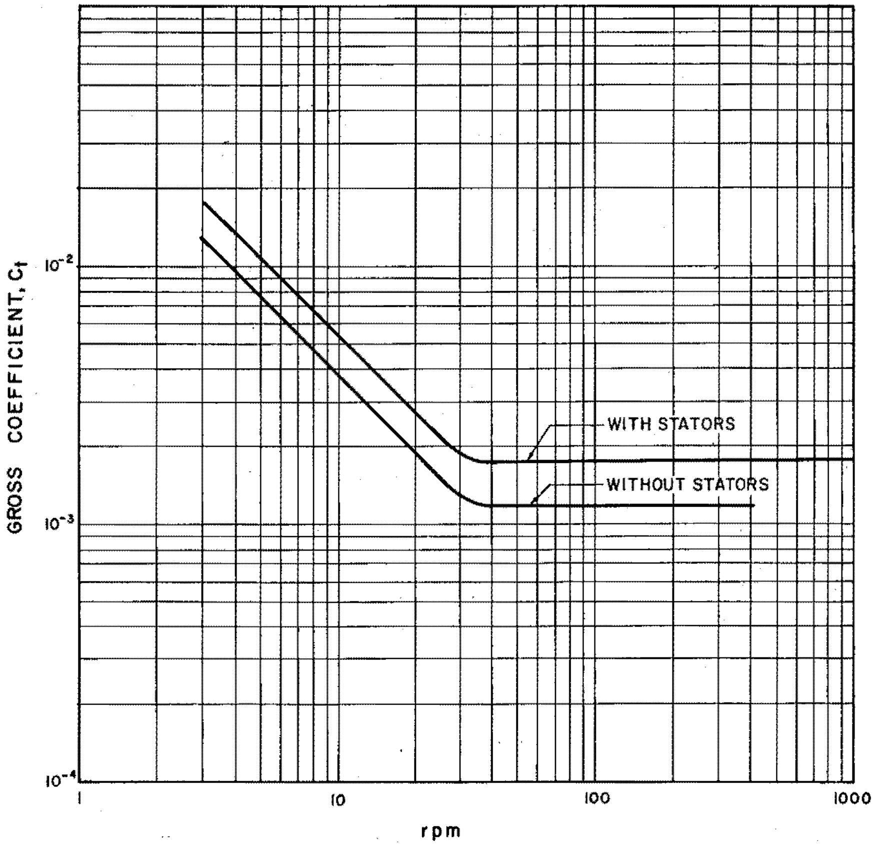

Fig. 4 — Gross drag coefficients for 4.4 in. sq. Rapid Mix Tank with water at 30°C.

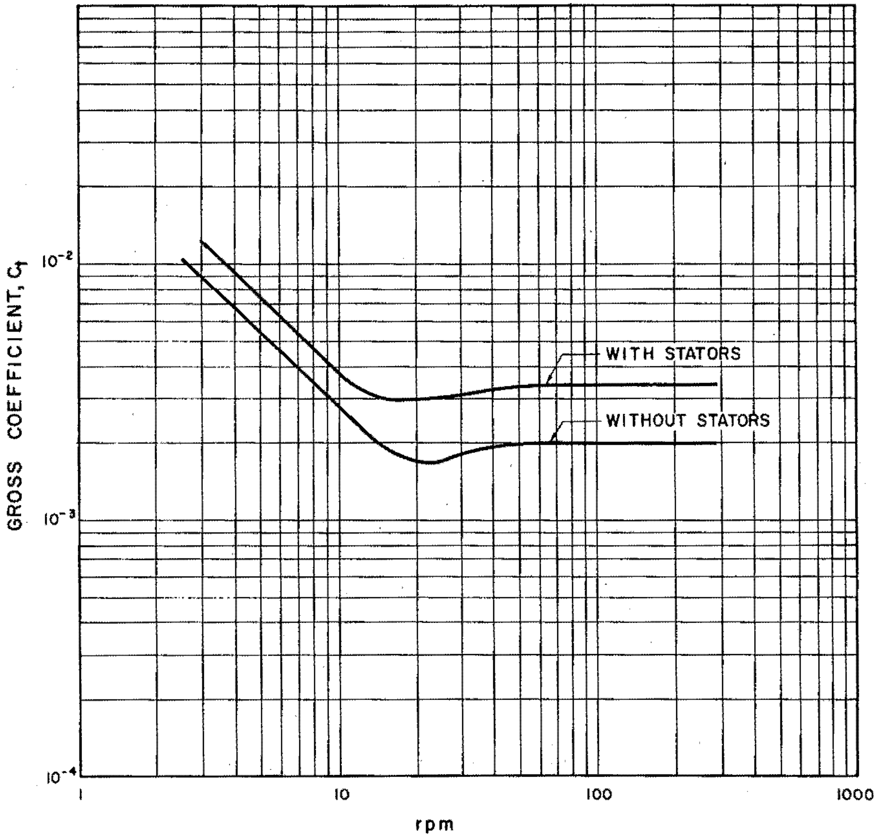

Fig. 5 — Gross drag coefficients for first 1 ft. sq. tank 3 ft. deep with water at 30°C.

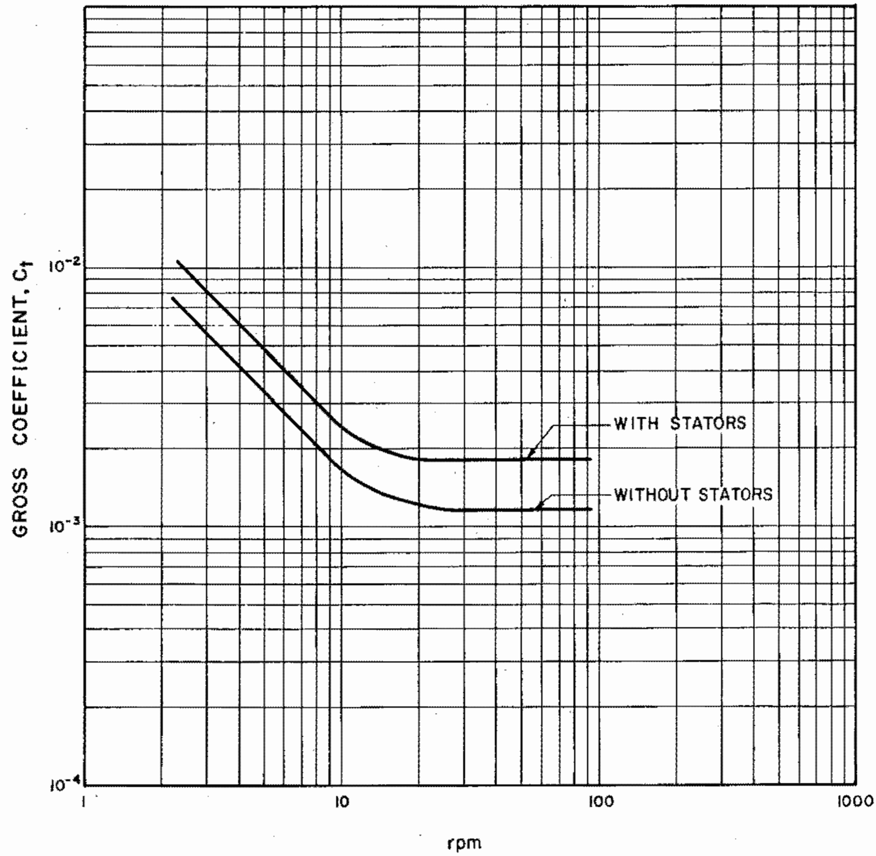

Fig. 6 — Gross drag coefficients for second 8 third 1 ft. sq. tank, 3 ft. deep, water at 30°C.

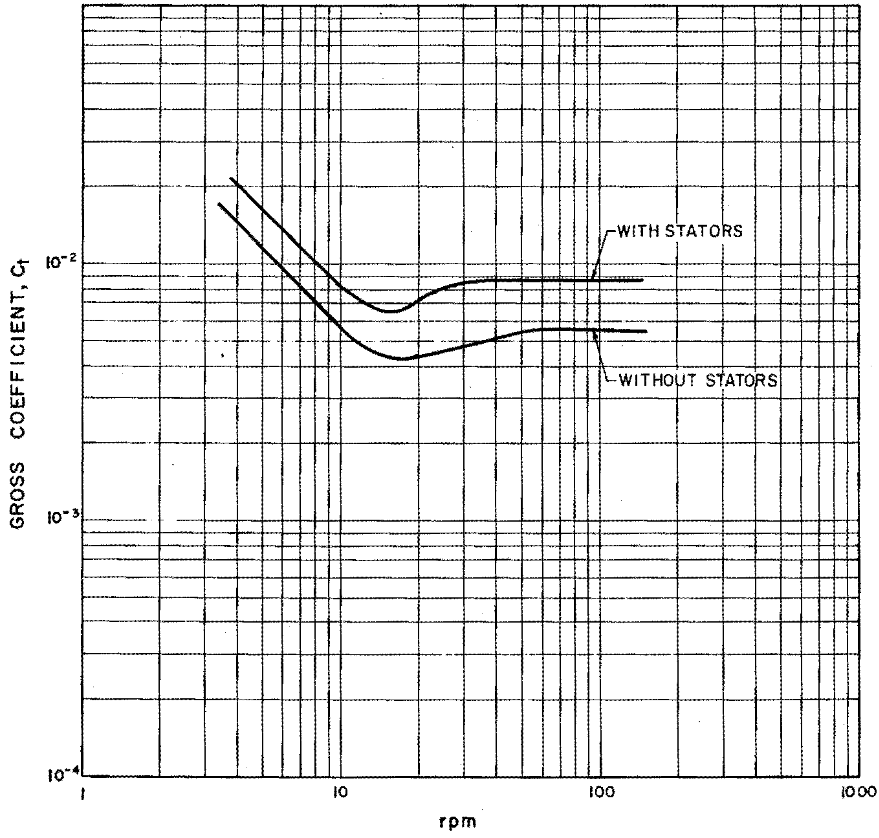

Fig. 7 — Gross drag coefficients for 1 ft. sq. tank 1 ft. deep with water at 30°C.

are 12 stators, placed in 4 groups of 3 each in the radial vertical planes through the corners with the inside edges 2.0 ft. from the center of the shaft. The stators are 3.0 ft. wide with the top and bottom stators 1.5 ft. high and the middle stators 2.0 ft. high. The dimensional moment parameters for turbulent drag, A_m, B_m and C_m are 114.2, 1752 and 7790 ft.[5], respectively; and for viscous drag, A_m', B_m' and C_m' are 0.0752×10^4, 2.17×10^4 and 179.2×10^4ft.[6], respectively.

For trial computations of the values of C_t for water at 30°C. on the turbulent and viscous tangents, the values of the drag and wall friction coefficients for the small cubical tank, column 5 of Table 1, will be used. For turbulent drag, f is assumed at 0.1072 and C_D at 1.469. For viscous drag, f′ is assumed at 0.01395×10^5 and C_D' at 5.23×10^5. For turbulent drag, the value of k_s, by Eq. (16), is 0.182 and the value of k is 0.31. From (7a), C_{t_s} is 4.85×10^{-3} and C_t is 3.47×10^{-3}. For viscous drag, by Eq. (24), k_s is 0.0276 and k is 0.1365. From (8a), C_{V_S} is 157.3 and C_V is 139.7. For 0.1 rpm, S is 1.667×10^{-3}; and from Eq. (6), C_{t_s} is 2.20×10^{-3} and C_t is 1.95×10^{-3}. The estimated positions of the tangents to the curves for C_t are shown by broken lines on Fig. 8.

For the proposed maximum value of W at 3.53 ft. lbs. per sec per ft.[3], the estimated speeds from Eq. (4) are 0.590 rps or 35.4 rpm with the stators, and 0.66 rps or 39.6 rpm without stators.

Acknowledgements

The author is indebted to his associates in Camp, Dresser & McKee for their assistance and cooperation, with special appreciation to Gerard F. Conklin, in charge of the research laboratory, for construction of the mixing equipment for the pilot plant and for torque and speed measurements and calculations. The author also acknowledges with thanks the assistance of Michael A. Collins, assistant engineer, in the calibrations and calculations.

REFERENCES

1. Camp, Thomas R. and Stein, Philip C., Velocity Gradients and Internal Work in Fluid Motion, *Journal of Boston Society of Civil Engineers,* October 1943, p. 219-237.
2. Stokes, G.G., On the Theories of Internal Friction of Fluids in Motion, Etc., *Camb. Phil. Trans. tVIII* (1845).
3. Camp, Thomas R., Floc Volume Concentration, *Journal of American Water Works Association,* 60:656 (June, 1968).
4. Camp, Thomas R., Flocculation and Flocculation Basins, *Transactions of American Society of Civil Engineers,* 120 (1955), p. 1-16.
5. Uhl, V. W. and Gray, J.B., *Mixing - Theory and Practice,* Academic Press, Inc., New York, 1966, Vol. 1, Chap. 4.
6. Hoerner, Signard F., *Fluid Dynamic Drag,* p. 3-16, Midland Park, New Jersey, 1965. Library of Congress No. 64-19666.

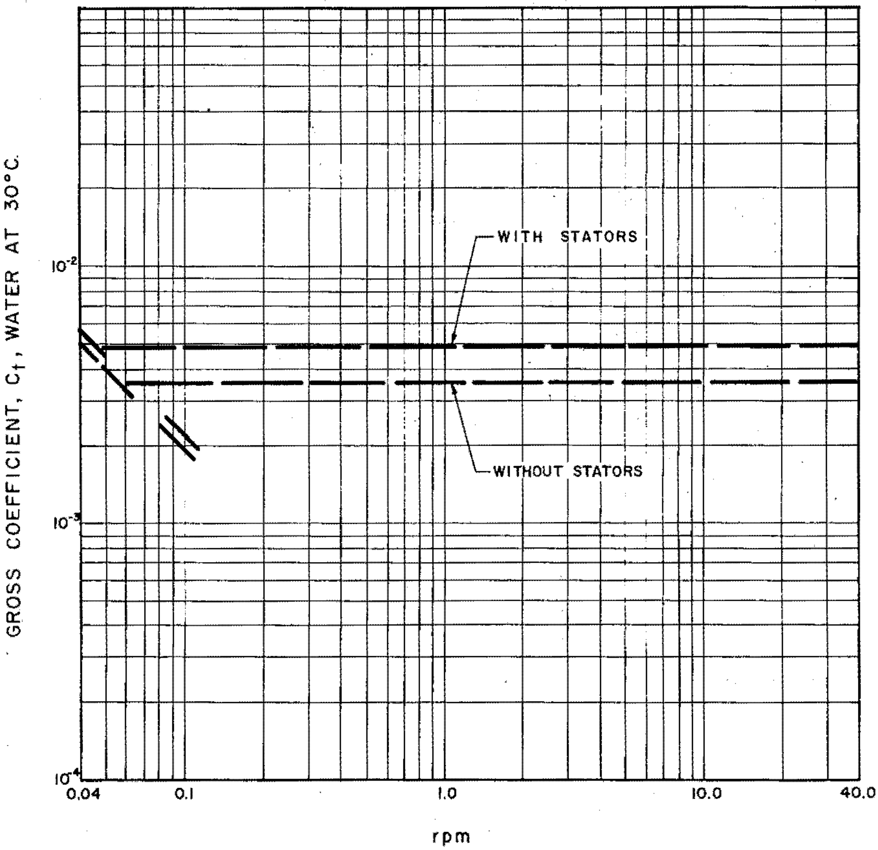

Fig. 8 — Estimated position of tangents to curves for gross drag coefficients for Billerica, (Mass.) rapid mix.

APPENDIX
Dimensional Parameters

The dimensional parameters for the rotors and stators are functions of the projected blade areas perpendicular to the direction of tangential flow and of the radii which determine the velocity and drag moments. As indicated on Fig. 2, the velocity is assumed to increase from zero at the center of the rotor shaft to a maximum at the tip of the radial rotor blade (or to the center of the outermost parallel rotor blade or outer edge for wide blades), and to remain constant from this point almost to the wall. The drag on the walls and floor is assumed to be the same per unit of wetted area and to be controlled by the maximum velocity at r_r ; and the drag moment arm is assumed to be r_w, the radius of circular tanks and the shortest radial distance to a wall for rectangular tanks. For simplicity, the total wall area is used for rectangular tanks with no allowance for corners.

Both radial rotors and wide blade parallel rotors and inside stators require integration of the differential moment and work on differential area, bdr, between r_1 and r_2. The moment arm to an outside stator is to its center, regardless of its width. Some stators may be partially inside and subjected to a velocity increasing with radial distance, and partially outside with constant velocity.

Wall Parameters

The drag per unit of wall area $= \rho \dfrac{fv^2}{8}$ (31)

For turbulent drag, the moment is (32)

$$M_w = \rho \frac{f}{4} A_w \frac{(2\pi)^2}{2} r_r^2 k^2 S^2 r_w = \frac{(2\pi)^2}{2} \rho C_D k^2 \frac{f}{C_D} (A_w \frac{r_r^2}{4} r_w) S^2$$

and the dimensional moment parameter is

$$C_m = A_w \frac{r_r^2}{4} r_w \tag{33}$$

Since the work is $M_w \dfrac{v}{r_w}$ or $M_w 2\pi \dfrac{r_r}{r_w} kS$,

$$W_w = \frac{(2\pi)^3}{2} \rho a \frac{C_D}{Va} k^3 \frac{f}{C_D} (A_w \frac{r_r^3}{4}) S^3 \tag{34}$$

and the dimensional work parameter is

$$C = A_w \frac{r_r^3}{4} \tag{35}$$

For viscous drag,

$$f = \frac{f'}{R} = \frac{f'\nu}{v4R} = \frac{f'\nu A_w}{v4V} \tag{36}$$

Substituting this value of f in (31), the viscous drag per unit of wall area

$$= \frac{f' \nu A_W}{v4V} \frac{\rho v^2}{8} = \frac{f'}{32} \mu \frac{A_W}{V} v \tag{37}$$

and viscous drag moment is

$$M_W' = \frac{f'}{32} \mu \frac{A_W^{\ 2}}{V} v r_W = \frac{f'}{32} \mu \frac{A_W^{\ 2}}{V} (2\pi r_r kS) r_W$$

$$= \frac{2\pi}{8} \mu \frac{C_D'}{V} k \frac{f'}{C_D'} (A_W^{\ 2} \frac{r_r}{4} r_W) S \tag{38}$$

and the dimensional moment parameter is

$$C_m' = A_W^{\ 2} \frac{r_r}{4} r_W \tag{39}$$

Since the work is $M_W' \frac{v}{r_W}$ or $M_W' 2\pi \frac{r_r}{r_W} kS$,

$$W_W = \frac{(2\pi)^2}{8} \mu \frac{C_D'}{V^2} k^2 \frac{f'}{C_D'} (A_W^{\ 2} \frac{r_r^{\ 2}}{4}) S^2 \tag{40}$$

and the dimensional work parameter is

$$C' = A_W^{\ 2} \frac{r_r^{\ 2}}{4} \tag{41}$$

Rotor Parameters

The turbulent drag per unit of projected blade area $= C_D \rho \frac{v^2}{2}$ (42)

The turbulent moment for narrow parallel rotors is

$$M_{pr} = C_D A_p \rho \frac{v^2}{2} r_p = \frac{(2\pi)^2}{2} \rho C_D (1-k)^2 (A_p r_p^{\ 3}) S^2 \tag{43}$$

and the dimensional moment parameter is

$$A_m \text{ per pr} = A_p r_p^{\ 3} \tag{44}$$

Since the work is $M_{pr} \frac{v}{r_p}$ or $M_{pr} 2\pi \frac{r_p}{r_p} (1-k) S$,

$$W_{pr} \text{ per pr} = \frac{(2\pi)^3}{2} \rho a \frac{C_D}{Va} (1-k)^3 (A_p r_p^{\ 3}) S^3 \tag{45}$$

and the dimensional work parameter is

$$A \text{ per pr} = A_p r_p^{\ 3} \tag{46}$$

which is the same as the moment parameter.

The turbulent moment for wide rotors, including radial rotors, is

$$M_{wr} = C_D b \int dr \rho \frac{v^2}{2} r = \frac{(2\pi)^2}{2} \rho C_D (1-k)^2 (b \int r^3 dr) S^3 \tag{47}$$

and the dimensional moment parameters are

$$A_m \text{ per rr} = b\int_0^{r_r} r^3\,dr = A_r\frac{r_r^3}{4} \tag{48}$$

and

$$A_m \text{ per wr} = b\int_{r_1}^{r_2} r^3\,dr = A_{wr}\frac{r_2^3 + r_2^2 r_1 + r_2 r_1^2 + r_1^3}{4} \tag{49}$$

Since the work is

$$M_{wr}\frac{V}{r} \text{ or } M_{wr}\,2\pi(1-k)\,S,$$

$$W_{wr} \text{ per wr} = \frac{(2\pi)^3}{2}\,\rho a\,\frac{C_D}{Va}\,(1-k)^3\,(b\int r^3\,dr)\,S^3 \tag{50}$$

and the dimensional work parameters are the same as the moment parameters as given by (48) and (49).

The viscous drag per unit of projected blade area =

$$\frac{C_D'}{R}\,\rho\frac{v^2}{2} = \frac{C_D'\nu}{v4R}\,\rho\frac{v^2}{2} = \frac{C_D'}{8}\,\mu\frac{A}{V}\,v \tag{51}$$

The viscous drag moment for parallel rotors is

$$M_{pr}' = \frac{C_D'}{8}\,\mu\frac{A_p^2}{V}\,v\cdot r_p = \frac{2\pi}{8}\,\mu\frac{C_D'}{V}\,(1-k)\,(A_p^2 r_p^2)\,S \tag{52}$$

and the dimensional moment parameter is

$$A_m' \text{ per pr} = A_p^2 r_p^2 \tag{53}$$

Since the work is $M_{pr}'\frac{V}{r_p}$ or $M_{pr}'\,2\pi(1-k)\,S,$

$$W_{pr}' \text{ per pr} = \frac{(2\pi)^2}{8}\,\mu\frac{C_D'}{V}\,(1-k)^2\,(A_p^2 r_p^2)\,S \tag{54}$$

and the dimensional work parameter is $A' \text{ per pr} = A_p^2 r_p^2$ (55)

which is the same as the moment parameter in (53).

The viscous drag moment for wide rotors, including radial rotors is

$$M_{wr}' = \frac{C_D'}{8}\,\mu\frac{A}{V}\,b\int dr\,vr = \frac{2\pi}{8}\,\mu\frac{C_D'}{V}\,(1-k)\,(Ab\int r^2\,dr)\,S \tag{56}$$

and the dimensional moment parameters are

$$A_m' \text{ per rr} = A_r b\int_0^{r_r} r^2\,dr = A_r^2\,\frac{r_r^2}{3} \tag{57}$$

and

$$A_m' \text{ per wr} = A_{wr} b\int_{r_1}^{r_2} r^2\,dr = A_{wr}^2\,\frac{r_2^2 + r_2 r_1 + r_1^2}{3} \tag{58}$$

The dimensional work parameters A′ per rr and per wr have the same values as the moment parameters in (57) and (58).

The values of the total rotor parameters for a mixing tank are summations of the individual rotor parameters, as follows.

The turbulent moment parameter or work parameter is

$$A_m = A = \sum A_p r_p^{\,3} + \sum A_r \frac{r_r^{\,3}}{4} + \sum A_{wr} \frac{r_2^{\,3} + r_2^{\,2} r_1 + r_2 r_1^{\,2} + r_1^{\,3}}{4} \quad (59)$$

and the viscous moment and work parameters are

$$A_m' = A = \sum A_p^{\,2} r_p^{\,2} + \sum A_r^{\,2} \frac{r_r^{\,2}}{3} + \sum A_{wr}^{\,2} \frac{r_2^{\,2} + r_2 r_1 + r_1^{\,2}}{3} \quad (60)$$

In computing values of the parameters, the terms in (59) and (60) which are not applicable are omitted.

The parallel rotor term may be used for wide rotors if r_2 is not greater than $1.5r_1$. For turbulent drag, the value of $r_p^{\,3}$ is 3.7% less than

$$\frac{r_2^{\,3} + r_2^{\,2} r_1 + r_2 r_1^{\,2} + r_1^{\,3}}{4}$$

for $\frac{r_2}{r_1}$ of 1.5 and 10% less for $\frac{r_2}{r_1}$ of 2.0. For viscous drag, the value of $r_p^{\,2}$ is 1.2% less than $\frac{r_2^{\,2} + r_2 r_1 + r_1^{\,2}}{3}$ for $\frac{r_2}{r_1}$ of 1.5 and 3.4% less for $\frac{r_2}{r_1}$ of 2.0.

Stator Parameters

Using the turbulent drag of (42), the turbulent moment for inside narrow stators and outside stators of width less than $r_w - r_r$ is

$$M_s = C_D A_s \rho \frac{v^2}{2} (r_{is} \text{ or } r_{os}) = \frac{(2\pi)^2}{2} \rho C_D k^2 (A_s r_{is}^{\,3} \text{ or } A_s r_r^{\,2} r_{os}) S^2 \quad (61)$$

and the dimensional moment parameter and work parameter for the inside narrow stators is

$$B_m \text{ per is} = B \text{ per is} = A_s r_{is}^{\,3} \quad (62)$$

The dimensional moment parameter for the outside stator is

$$B_m \text{ per os} = A_s r_r^{\,2} r_{os} \quad (63)$$

Since the work is $M_s \frac{v}{r_{os}}$ or $M_s\, 2\pi \frac{r_r}{r_{os}} k\,S$, the dimensional turbulent work parameter for the outside stator is

$$B \text{ per os} = A_s r_r^{\,3} \quad (64)$$

For wide inside stators,

$$B_m \text{ per is} = B \text{ per is} = A_s \frac{r_2^3 + r_2^2 r_1 + r_2 r_1^2 + r_1^3}{4} \tag{65}$$

Using the viscous drag of (51), the viscous drag moment for inside narrow stators and for outside stators is

$$M_s' = \frac{2\pi}{8} \mu \frac{C_D'}{V} k (A_s^2 r_{is}^2 \text{ or } A_s^2 r_r r_{os}) S \tag{66}$$

and the dimensional moment parameter and work parameter for the inside narrow stators is

$$B_m' \text{ per is} = B \text{ per is} = A_s^2 r_{is}^2 \tag{67}$$

The dimensional moment parameter for the outside stator is

$$B_m' \text{ per os} = A_s^2 r_r r_{os} \tag{68}$$

and the work parameter is

$$B' \text{ per os} = A_s^2 r_r^2 \tag{69}$$

For wide inside stators,

$$B_m' \text{ per is} = B \text{ per is} = A_s^2 \frac{r_2^2 + r_2 r_1 + r_1^2}{3} \tag{70}$$

The values of the total stator parameters for a mixing tank are summations of the individual stator parameters, as follows.

The turbulent moment parameter is (71)

$$B_m = \sum A_s r_{is}^3 + \sum A_s r_r^2 r_{os} + \sum A_s \frac{r_2^3 + r_2^2 r_1 + r_2 r_1^2 + r_1^3}{4}$$

and the turbulent work parameter is (72)

$$B = \sum A_s r_{is}^3 + \sum A_s r_r^2 r + \sum A_s \frac{r_2^3 + r_2^2 r_1 + r_2 r_1^2 + r_1^3}{4}$$

The viscous moment parameter is (73)

$$B_m' = \sum A_s^2 r_{is}^2 + \sum A_s^2 r_r r_{os} + \sum A_s^2 \frac{r_2^2 + r_2 r_1 + r_1^2}{3}$$

and the vicous work parameter is (74)

$$B' = \sum A_s^2 r_{is}^2 + \sum A_s^2 r_r^2 + \sum A_s^2 \frac{r_2^2 + r_2 r_1 + r_1^2}{3}$$

In computing values of the parameters, the terms which are not applicable are omitted.

The parallel stator term may be used for wide inside stators if r_2 is not greater than $1.5 r_1$. The error in using the simpler term is the same as shown above for rotors.

PROPOSED ALCOSAN SECONDARY TREATMENT

by

GEORGE T. GRAY*, ARIEL A. THOMAS**, Member
and JOHN F. DENNIS***

(Paper presented at a meeting of the Sanitary Section, Boston Society of Civil Engineers on December 4, 1968.)

Background

The Allegheny County Sanitary Authority was organized in 1946 to comply with the Clean Streams Act passed by the Pennsylvania Legislature in 1945. This Act required all municipalities and industries to cease the discharge of untreated wastes into the streams of the Commonwealth. The Authority is known as "Alcosan". Metcalf & Eddy, Inc. has been consultant to Alcosan since 1947.

Alcosan now serves 72 municipalities plus the City of Pittsburgh. The collection system includes 69 miles of interceptors varying from 10½ ft diameter at the main pumping station at the treatment plant down to 8 in. and 12 in. connecting sewers throughout the system. It generally follows the banks of the three rivers and two large creeks, and is almost entirely gravity flow with the exception of three small pumping stations and three ejector stations. Approximately 30 miles of the collection system is in deep rock tunnel. The collection systems of individual municipalities discharge into, but are not part of, the Alcosan system.

The present treatment process is termed intermediate because of the preaeration channels, but is actually little better than primary treatment. In general, the plant consists of a main pumping station, rack and chlorination building, grit channels, meter vault, preaeration channels and sedimentation tanks, sludge heating facilities, sludge concentration tanks, and incinerators.

All of the existing plant is designed for a peak flow of 300 mgd. All but the primary settling tanks are designed for an average daily flow of 200 mgd. The primary settling tanks are designed for an average daily flow of 150 mgd. However, space was provided in the original design for two additional primary tanks if they should be required by regulatory agencies. The sludge disposal at the present time is by heating, sludge concentration by anaerobic flotation (Laboon process), and flash-drying incineration. The concentrated sludge averages 16 percent solids.

The collection system and treatment plant took 3 years to construct

**Chief Engineer*, Allegheny County Sanitary Authority.
***Senior Vice President*, Metcalf & Eddy, Inc.
****Project Manager*, Metcalf & Eddy, Inc.

and was placed in operation in June 1959. The total cost for engineering, financing and construction was approximately 100 million dollars. The treatment plant cost was approximately $20,000,000.

Future Requirements

In 1965 and 1966, Alcosan and the State Sanitary Water Board held several meetings to discuss new and improved treatment not contemplated by either in the original project. The State Sanitary Water Board issued an order on March 16, 1966 requiring Alcosan to provide additional wastewater treatment. The Authority cooperated by submitting a schedule for reports, plans and specifications, and construction, and has met this schedule to date. Nine years after Alcosan's intermediate wastewater treatment plant was placed in operation, Metcalf & Eddy completed plans and specifications for secondary treatment and additional sludge disposal facilities in order to meet more stringent stream standards and upgraded effluent requirements. The State Sanitary Water Board has approved the plans and issued a permit for construction.

The estimated construction cost of the project is $38,500,000 with a project cost of $49,700,000. Alcosan has applied for federal and state construction grants. If a grant of at least 30 percent is made, construction may start in the spring of 1969, and may be completed in 1970, all on schedule. The Authority needs a large construction grant in order to keep the increase in the service charge rate reasonable. Even with a 30 percent construction grant, the added operation, maintenance, and capital cost may require an increase in the service charge rates. The increased operation and maintenance costs alone are estimated at $1,255,000, about 33 percent of the present operation and maintenance budget.

Fig. 1 shows the population and accounts served. These have increased slowly in the past and, as can be seen, are expected to increase slowly in the future. It is noted that the rate of increase of population and accounts served are approximately the same. Alcosan's present policy is to admit no new participants inasmuch as the collection system is designed to handle only the wastewater flows from the present participants and can be expanded only at a great additional cost.

Fig. 2 shows the average annual wastewater treatment plant flow records and the future trend. Since the records show no trends, the flow has been projected generally in accordance with increases in the population and the numbers of accounts. We expect the average annual flow to increase from approximately 140 mgd to about 150 mgd by 1985.

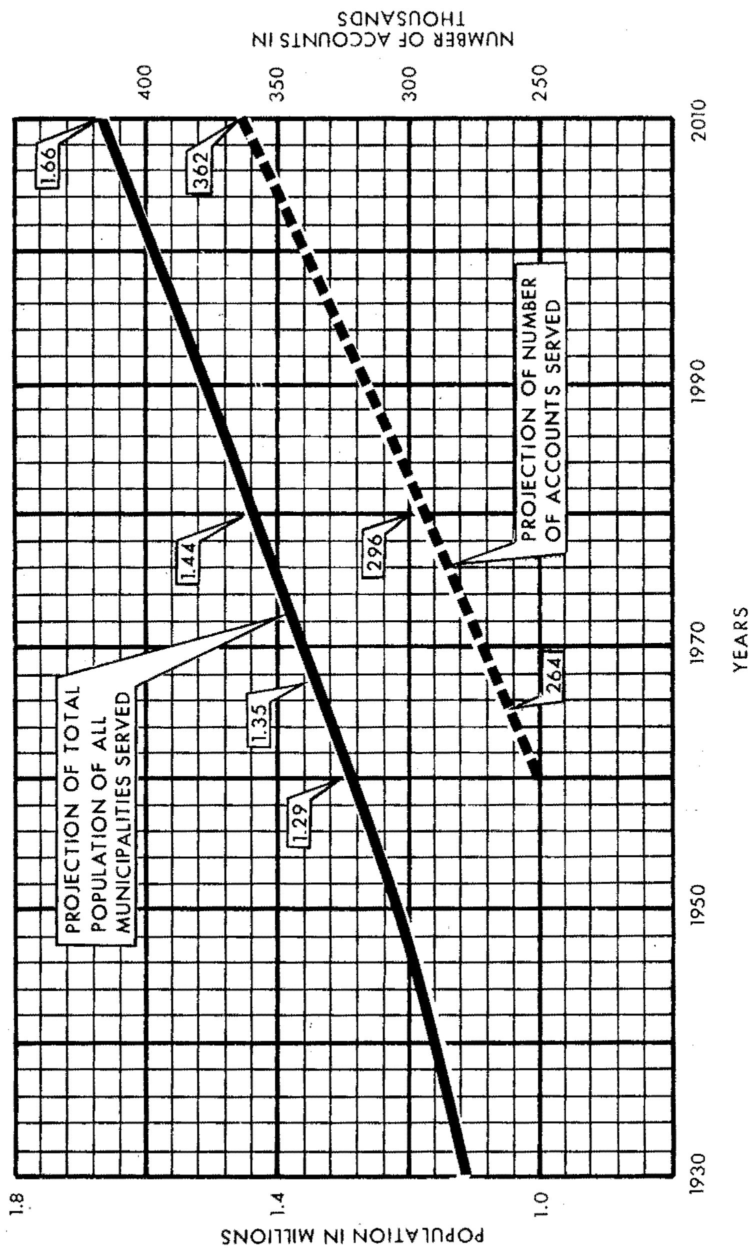

Fig. 1 — Population and accounts trends.

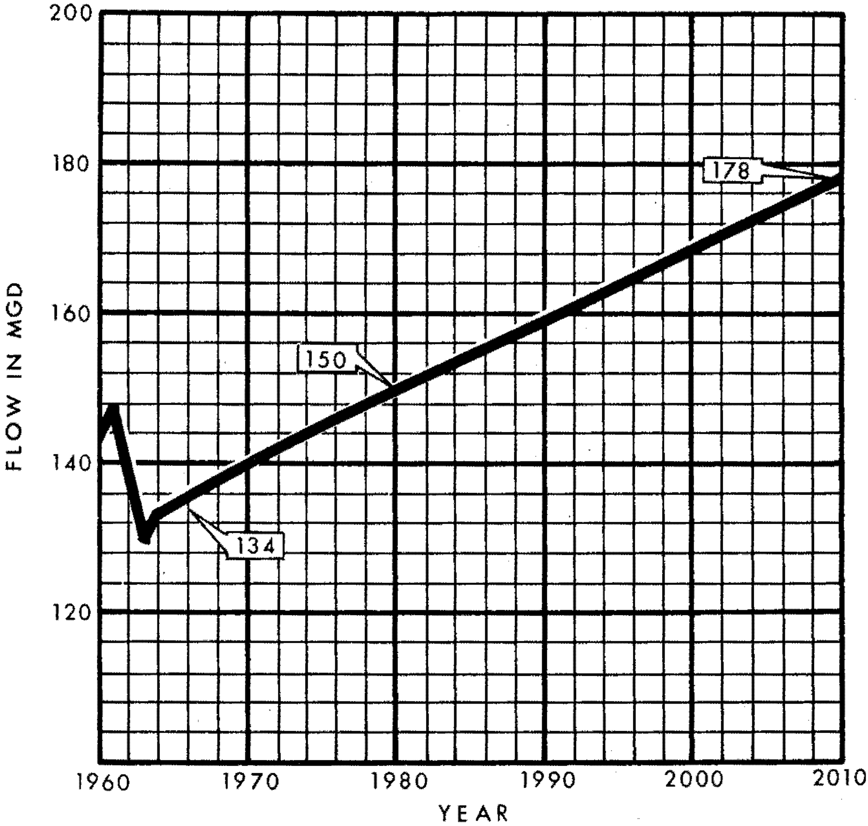

Fig. 2 — Waste water flow trend.

The Pennsylvania Sanitary Water Board order requires Alcosan to discharge less than 60,000 lb/day of 5-day, 20 deg C BOD into the Ohio River. Our computations showed that the Ohio River dissolved oxygen will be in excess of 4.0 mg/L downstream of the Alcosan outfall if not more than 90,000 lb of BOD are discharged into the river each day. In general, removal of 85 percent of the influent BOD is required if the project is to be considered for federal construction grants. We have designed for 90 percent BOD removal.

Fig. 3 shows estimated raw and effluent BOD in 1970 with the existing intermediate treatment, just before the new facilities are placed in operation, and for 1970, 1980, and 2010 with the new facilities in operation. In 2010, the BOD load into the river is expected to be one half of the load allowed by the Sanitary Water Board.

Proposed Secondary Facilities

The proposed plant additions will consist of six aeration tanks, 12 final settling tanks, and two chlorine contact tanks. The existing preaeration tanks will be bypassed and used for partial aerobic digestion of the waste-activated sludge. They can be kept in service as preaeration tanks, if desired. Sludge disposal will be by vacuum filtration and incineration of raw sludge. No additional primary settling tanks are planned up to the design flow of 200 mgd. Although the existing tanks are designed for only 150 mgd, the reduction in efficiency up to 200 mgd is slight and will be compensated for by the secondary treatment. Space has been reserved in this design for two additional tanks if they should be required in the future by the regulatory agencies.

Fig. 4 shows schematically the existing and proposed wastewater treatment. It is noted that preaeration will be eliminated and the tanks used for aerobic digestion of waste-activated sludge.

The six aeration tanks are diffused-air, spiral-flow tanks designed for an average daily flow of 150 mgd, and a design loading of 45 lb of BOD per 1,000 cu ft. It is expected that the loadings can easily be increased to 60 lb of BOD per day per 1,000 cu ft, and that the six tanks will treat an average daily flow of 200 mgd. The air capacity and hydraulic design are such that six aeration tanks will be able to treat an average daily flow of 200 mgd and a peak flow of 300 mgd. The present state standards for design loadings of aeration tanks permit not more than 35 lb of BOD per day per 1,000 cu ft of tank. The use of the 45-lb loading which was approved by the state reduced the size of the aeration tanks significantly. We are confident that op-

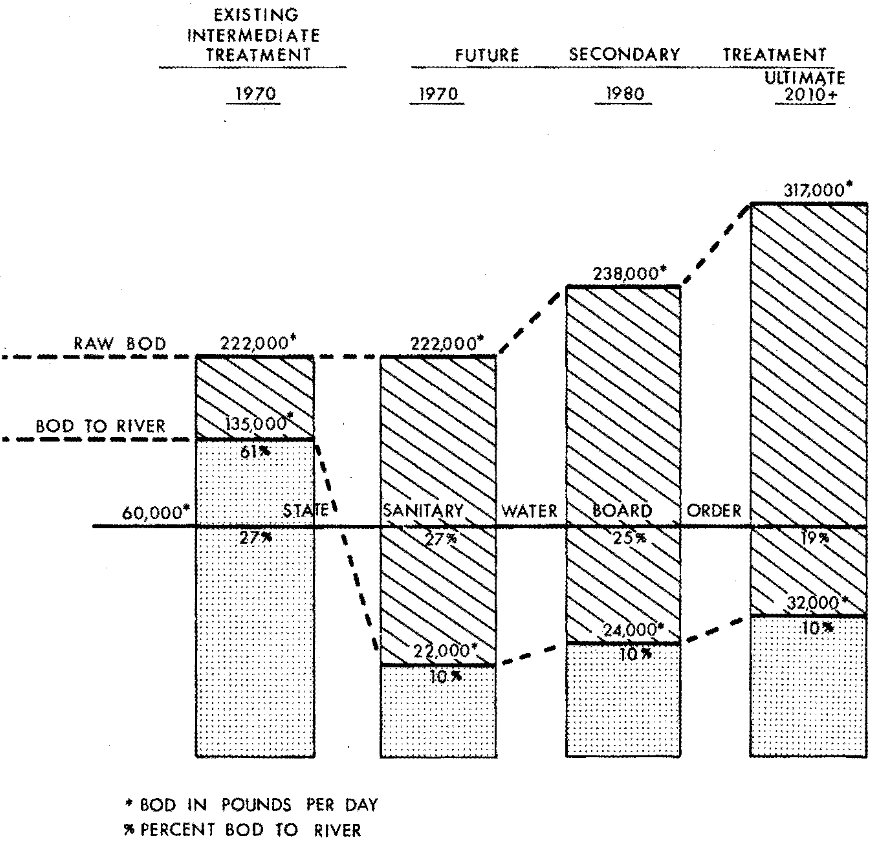

Fig. 3 — BOD information.

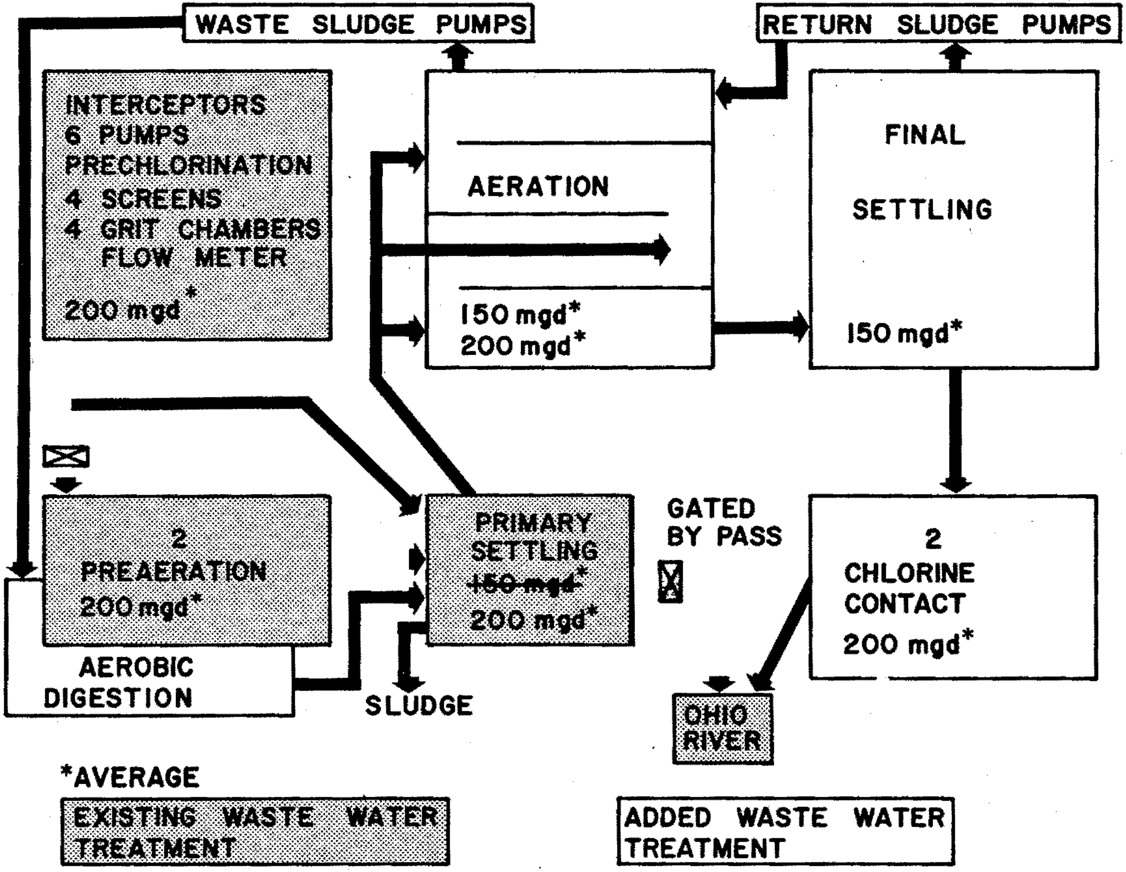

Fig. 4 — Waste water treatment.

eration will prove that the higher loadings of 60 lb of BOD per 1,000 cu ft will provide a 90 percent reduction, and that additional aeration tanks will not be required in the future. However, space was left for two additional aeration tanks if they are required.

The 12 circular final settling tanks, 141 ft in diameter, are designed on the basis of a 1,200-gallon per square foot per day overflow rate for a peak flow of 225 mgd. These tanks will have to be supplemented by two additional tanks as the peak flow increases from 225 mgd to 263 mgd, and by two more tanks as the peak flow increases from 263 mgd to 300 mgd. Space for the four additional tanks has been provided on the site.

The chlorine contact tanks are designed to provide a 15-minute detention at peak flows of 300 mgd.

It is believed that, by the addition of four final settling tanks, the existing and presently proposed sewage treatment plant can provide a 90 percent BOD removal for an average daily flow of 200 mgd and a peak flow of 300 mgd.

A blower building will contain four initially, and room for a fifth, centrifugal compressors, each having a capacity of 60,000 cu ft of air per minute. The air will be filtered through rough filters, electrostatic precipitators, and bag-type filters to reduce the tendency to clog the fine bubble tube diffusers that are specified.

A small new operations building will be constructed next to the blower building. Secondary treatment and final chlorination will be supervised from this building. It will contain a small laboratory for operation control tests; a center for the automatic control equipment; shower, locker, and lunch room facilities; and some storage space.

The operations building is electrically heated, as is the blower building. The large electrical use in the plant makes it economical to use electrical heating. Much of the heat for the blower building will be produced by the blowers themselves although supplemental electrical heat will be required when the number of blowers operating is not sufficient to maintain a reasonable temperature.

The new buildings and structures and existing plant facilities will be interconnected by tunnels and passageways so that the entire plant operation can be observed without going outside in inclement weather. Practically all wire and pipe are installed in tunnels and easily accessible. Most of the power and control wires will be laid in trays.

Sludge Disposal

The sludge disposal for the proposed treatment plant is shown diagrammatically on Fig. 5. It will consist of wasting activated sludge to the existing preaeration tanks, which will be used as aerobic digestion tanks. The partially-digested activated sludge will be discharged into the raw sewage and will be resettled with the raw sewage solids in the present primary settling tanks. The raw sludge containing waste-activated and primary sludge solids will be pumped from the primary tanks through disintegrators into mixing tanks. The sludge will then be pumped to vacuum filters, dewatered, and carried by belt conveyors to the existing incinerators. The incinerator ash will be settled together with residue from two-stage tray scrubbers in the existing ash settling tanks along the river wall. The supernatant from the ash settling tanks will be returned to the raw sewage for treatment. The ash will be handled as at the present time by hauling to a spoil area which the Authority maintains a couple of miles from the treatment plant.

The present incinerators were designed to incinerate sludge concentrated to 16 percent solids. The incinerators actually are evaporators of water, and were designed to evaporate water from sludge containing 84 percent water with the use of supplemental heat. The increased solids concentration in the vacuum filter cake, compared with the present concentrated sludge, will markedly increase the capacity of the incinerators to dispose of solids. Fig. 6 shows the amount of wet sludge which can be incinerated as the sludge solids increase from 16 percent solids to 20 percent solids to 25 percent solids. It is noted that a constant amount of water is being evaporated. Also significant is the marked increase in the pounds of dry solids which can be disposed of through a given incinerator.

The incinerators were plagued for years with deposits on the vapor fan blades, which required that the incinerators be taken off line and solids chipped from the blades at intervals as short as 5 days. Investigation and experimental work by the Authority has proven that a minimum temperature in the drying cycle of 300 deg F will prevent deposits on the vapor fans and will permit the vapor fans to operate almost indefinitely. Incinerator runs now exceed 1,000 hours, or 40 days. Therefore, while in the past it became difficult at times to keep two incinerators on line with a total of four available, three incinerators can now be used most of the time. As a result of the higher solids concentration in the vacuum filter sludge cake, and the solution of the vapor fan problem, the incinerators will have a capacity to handle the primary and secondary sludge from a 200 mgd flow.

Two-stage scrubbers will be added to the incinerators so they will meet the applicable county air pollution codes. The alternative would have been

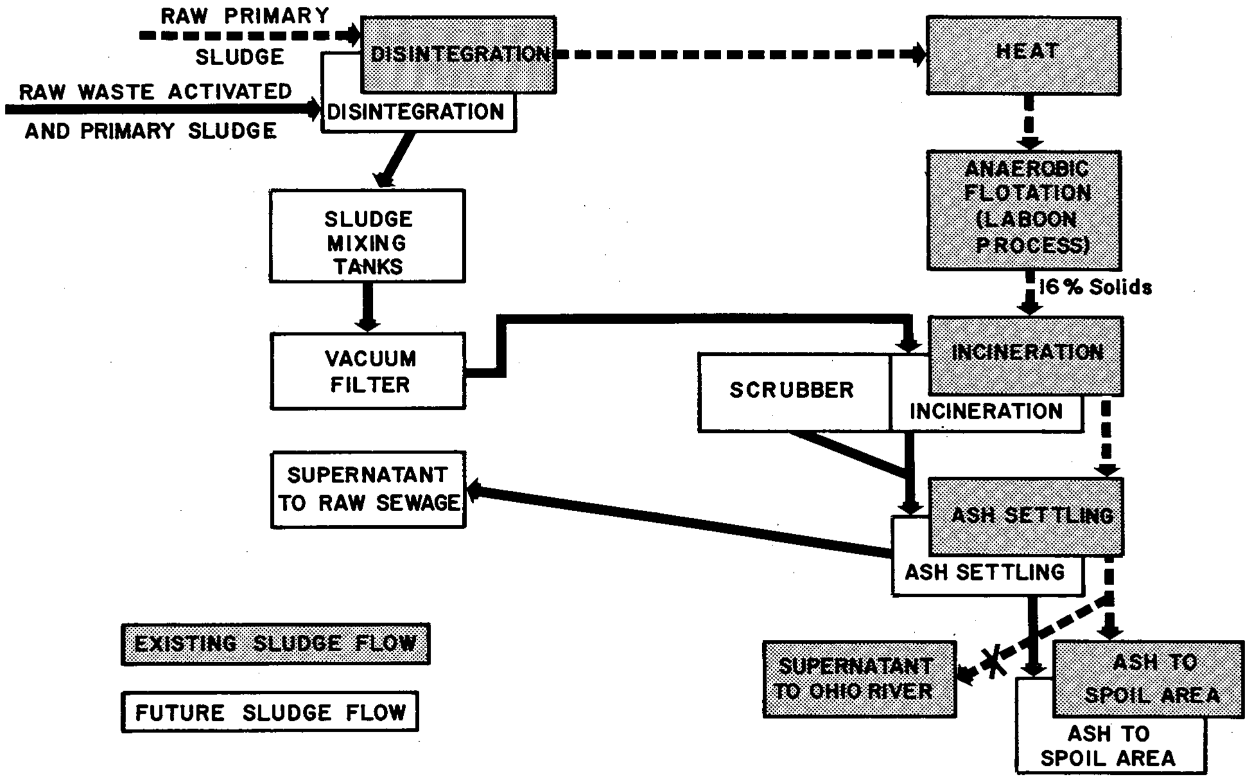

Fig. 5 — Sludge disposal.

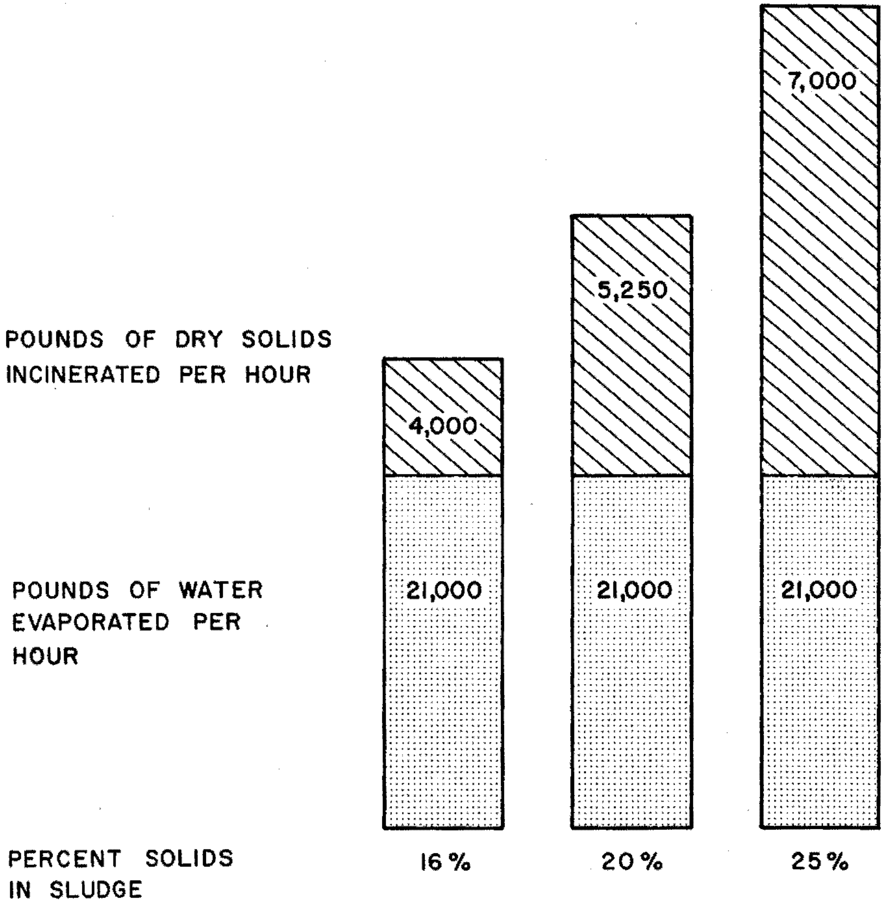

Fig. 6 — Incinerator capacity.

to scrap the existing incinerators and replace them with new incinerators which would give a satisfactory stack discharge into the atmosphere.

Design Features

A few of the interesting features of design are discussed below.

The secondary treatment facilities are designed so that they can be operated as two completely separate plants, or as one plant. Initially, the Authority staff will operate two completely separate plants. They will use different mixed liquor concentrations, dissolved oxygen concentrations, periods of sludge reactivation, points of wastewater application, and BOD loadings to find the optimum operating criteria. Inasmuch as the staff will apply different operating criteria to two portions of the same wastewaters, the operation results will be much more informative than if the different criteria were to be applied to different wastewaters on different days. Once the best ranges of operating criteria are determined, the secondary treatment facilities will probably be operated as a single plant.

The flows from one primary settling tank effluent channel will be discharged into the six, or fewer, aeration tanks. The flows will be measured and regulated by flowmeters and automatic controls so that the primary effluent can be divided evenly between the aeration tanks in operation, or can be divided 60 percent to one side of the plant and 40 percent to the other side of the plant if desirable during the investigations in early years, when the two sides of the secondary treatment plant are operated as two completely separate plants.

A plan of one aeration tank is shown on Fig. 7. It is noted that the sludge follows a U-shaped course. The re-aeration compartment is closest to the final settling tank. Primary effluent can be applied to each or any combination of the second, third, or fourth compartments. This configuration reduces the piping and channels which are required. The actual amount of sewage discharged to each one of the compartments is controlled by manually-operated gates.

Aeration will be automatically controlled. Each compartment of each aeration tank will have three points at which DO analyzers can be installed. Only one DO analyzer is expected to be installed in each compartment of each tank. The best location for control of dissolved oxygen must be determined in the field. In the early stages of operation the DO analyzers will be moved among the three points to find the best location to measure and control the dissolved oxygen. Dissolved oxygen in each of the four compartments of the aeration tank will be controlled separately. The dissolved oxy-

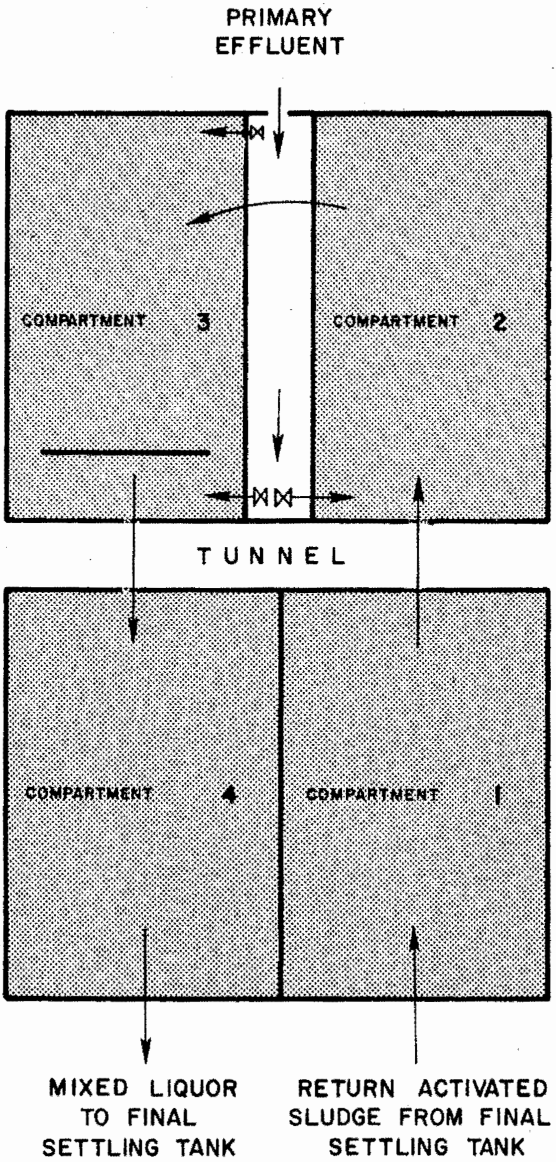

Fig. 7 — Plan of one aeration tank.

gen measured by the DO meter in one compartment will control a butterfly valve in the air header serving that compartment of the aeration tank. The butterfly valve will be controlled in such a way that the minimum discharge to any one section of tank will be kept above the minimum required to keep the tank contents completely mixed. Inasmuch as there are six tanks and four compartments in each tank, this will require 24 dissolved oxygen analyzers and 24 air control points.

The blowers will be automatically controlled to produce the correct amount of air. The control will be based on the blower discharge pressures, which will change as the butterfly valves on the air supply pipes to each compartment open and close to meet the demands for air. This system will provide only the air required to maintain the dissolved oxygen at the optimum level in each compartment. Power saving from supplying just enough air, and better treatment from always supplying enough air, are expected.

The coliform effluent standards permit only 5,000 coliforms per 100 ml. The rate of postchlorine feed will be automatically controlled by a chlorine residual meter to produce a residual chlorine which will reduce the coliforms to the required level. Postchlorination of approximately 10 mg/L will be required.

Fig. 8 "Effluent Chlorination Control" shows that chlorine will be fed into the final settling tank effluent channels immediately ahead of a rapid-mixing chamber. A sample of chlorinated wastewater is taken immediately after the rapid-mixing chamber and pumped to a chlorine residual meter. The chlorine residual reading is transmitted to the chlorinator controller which increases or decreases the rate of chlorine feed to meet the set-point residual. The required residual will probably be in the neighborhood of 5.0 mg/L for the disinfection required. The actual required residual will be determined by comparing coliform counts at the effluent end of the chlorine contact tank with the set-point residual. The set-point residual will be adjusted daily, and then weekly, until a residual is found which will produce a plant effluent containing no more than 5,000 coliforms per 100 ml. Automatic control of chlorination not only saves chlorine but is also more effective.

Prechlorination will be retained and is expected to be used in the summertime to control hydrogen sulfide odors from the raw sewage. Approximately 5 mg/L will probably be used during the warm weather for this purpose.

Experience has shown that sludge disintegrators are very important to the trouble-free operation of plunger sludge pumps. Therefore disintegra-

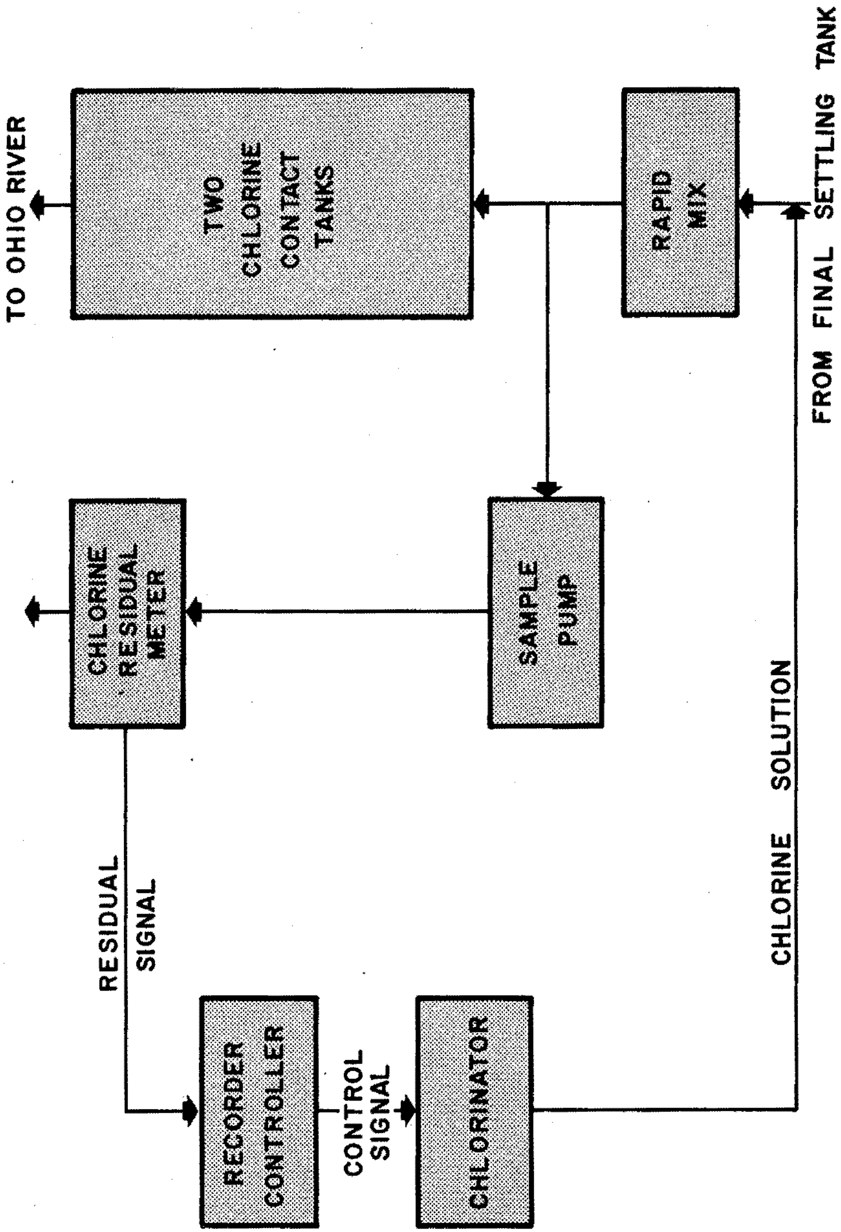

Fig. 8 — Effluent chlorination control.

tors will be provided before the mixture of primary and waste-activated solids is discharged into the mixing tanks. These two mixing tanks are essentially wide places in the sludge lines, with capacity to handle approximately six hours of sludge flow. Mixing will be accomplished with slow-speed mixers to prevent any rapid change in sludge concentration or characteristics. The tanks will also serve as suction wells for the duplex plunger pumps which will pump sludge to the vacuum filters.

Each vacuum filter will be fed by one plunger pump. The plunger pump speed will be controlled by the level in the filter tank.

Facilities are being provided so that sludge can be conditioned with two polymers or with one polymer and ferric chloride. No provision has been made for the use of lime in the conditioning of the sludge. The operator will proportion the amount of each conditioning chemical fed to each filter, and control equipment will automatically maintain this proportion as the sludge pump speed varies to maintain the sludge level in the filter tank.

One console will control four vacuum filters. The filter drum speed will be variable and remotely controlled from the console. Valves are provided on both the pickup line and the drying vacuum line. Each vacuum filter will have its own vacuum pump and its own chemical-feed pumps. In general, each filter will operate completely separately and have completely separate auxiliary equipment. If any part of a filter or its auxiliary equipment requires maintenance, the filter will be taken out of operation and a spare filter placed in operation.

Carbon filters will be used to remove sludge odors from all air which will be discharged to the outside of the vacuum filter building, or recirculated. Two sets of filters will be included, one to take care of the general area, and one to take care of the gases which are pulled out of the filter by the vacuum pumps.

Conclusion

The proposed Alcosan secondary wastewater treatment plant will be a modern semi-automatic facility which will provide a high degree of treatment. It, in conjunction with wastewater treatment facilities to be built by other municipalities and industries, will assure excellent conditions in the Ohio River for years to come.

HEAD LOSSES CAUSED BY AN ICE COVER ON OPEN CHANNELS

PETER A. LARSEN*, *Member*

(Paper presented at a meeting of the Hydraulics Section, Boston Society of Civil Engineers, on November 2, 1966)

Introduction

The design of open channels in areas with long-lasting cold winters requires consideration of various types of ice problems. One such problem is the effect of an ice cover on head losses. The increase of head losses in, for instance, a hydro-power channel is directly proportional to a reduction in power production. In wintertime the value of the power generated would be generally greater than in the warmer periods of the year. The economical aspect is therefore obvious and the question is: What is the cross sectional channel area that will give optimum economy?

Two types of information are necessary for channel design:

1.) Knowledge of the roughness of the ice cover.

2.) A method of computing the effect of the composite roughness of a given channel, the bottom and ice roughness being known.

Very little can be found in the hydraulic literature about ice roughness. Some authors recommend that the same friction factor be used for the ice cover as for the channel bottom. Others suggest that the ice cover be considered as a hydraulically smooth surface. Of these suggestions the latter might appear to be the more logical, but it will be shown that this assumption is generally too optimistic.

As far as the composite roughness is concerned, a variety of formulas can be found based on different assumptions. As pointed out by Ven Te Chow some of these result in negative friction factors for the ice cover, an illogical result.[1]

The aim of this paper is to develop a rational formula for composite roughness based on the concept of logarithmic velocity distribution, and to report some field data relative to the roughness of the ice cover on two different Swedish power channels. The field data provided a check on the deduced formula.

---

*Associate Professor, Worcester Polytechnic Institute, Worcester, Massachusetts.

1. Chow, Ven Te: Open Channel Hydraulics, 1959.

Formation of Ice Covers

In areas with cold climate, it is generally desirable to have an ice cover on the channels. This prevents the production of so-called frazil ice which generally results in the formation of hanging dams or anchor ice with uncontrollable, high head losses.

An ice cover is known to form in either one of two ways. The one dealt with here is the formation similar to the ice covering on a lake. This type of ice cover can form only when the flow velocity is relatively low- less than 2 fps. Such an ice cover is, however, known to be stable at considerably higher velocities than those at which it can be formed. This is due to the fact that the whole flow pattern is changed when the cover is present. The ice forms a rigid boundary and consequently the flow velocity is zero at the ice surface and the maximum velocity occurs somewhere near mid-depth.

An ice cover may also be built up by floating ice which is transported by the flowing stream and deposited at the edge of an ice cover that has formed in a low velocity zone of the channel. Such an ice cover is known to have a relatively high initial resistance coefficient which tends to decrease with time.[2] However, the roughness of the ice cover considered here has been shown to increase with time.

In an investigation made by the Swedish State Power Board, ice floes were sawn out of the ice cover on two different power plant supply channels. Figures 1 to 6 show the under side of the ice floes. A wavy pattern is apparent with its main direction being perpendicular to the direction of flow. A floe with its orientation perpendicular to the direction of flow did not show a regular wave pattern, although the surface was not smooth. The channel characteristics of the floes shown in Figures 1 to 3 were: depth about 13 feet, width roughly 300 feet, and the velocity of flow varying between 0 and 2.3 fps depending on short term regulation of the power station.

The floes shown in Figures 4 to 6 formed on a channel with somewhat different characteristics: depth about 35 feet, width 200 feet, flow velocities varying between 0 and 4.0 fps, and a short-term regulated flow. Temperature measurements in this channel showed that the water temperature was constant at all depths, with a value of 0.01 C° measured at different locations along the channel.

To get an idea of the development of the surface configuration with time, an ice floe with a smooth upper side was turned and left in this

2. R. Beccat and B. Michel: International Association for Hydraulic Research, Proceedings 1959, Vol. III.

Fig. 1 — Ice floes from the Alvkarleby Head Race canal.

Fig. 2 — Ice floes from the Alvkarleby Head Race canal.

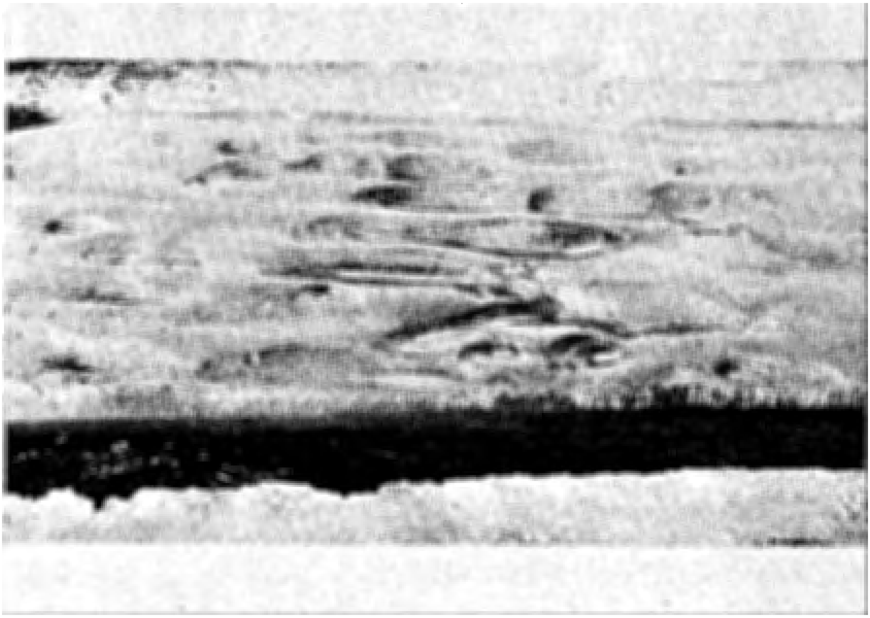

Fig. 3 — Ice floes from the Alvkarleby Head Race canal.

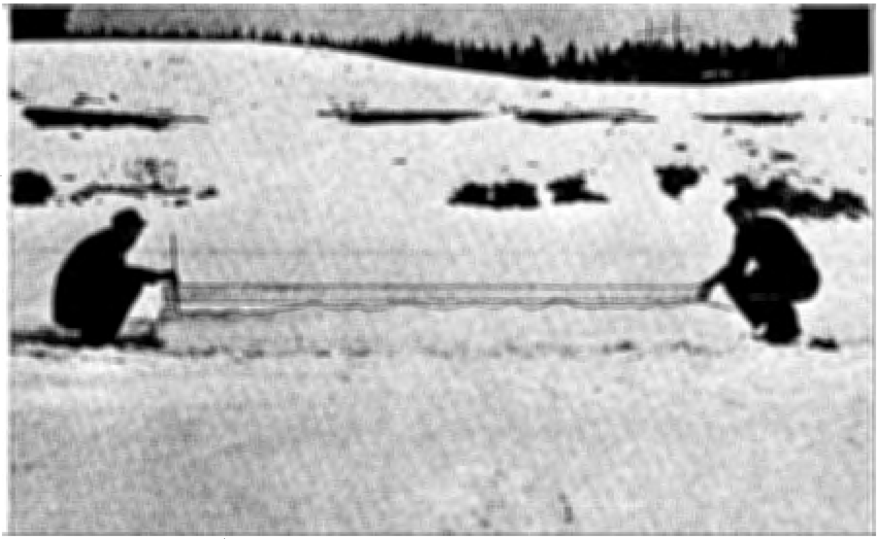

Fig. 4 — Ice floes from the Kilforsen Power canal.

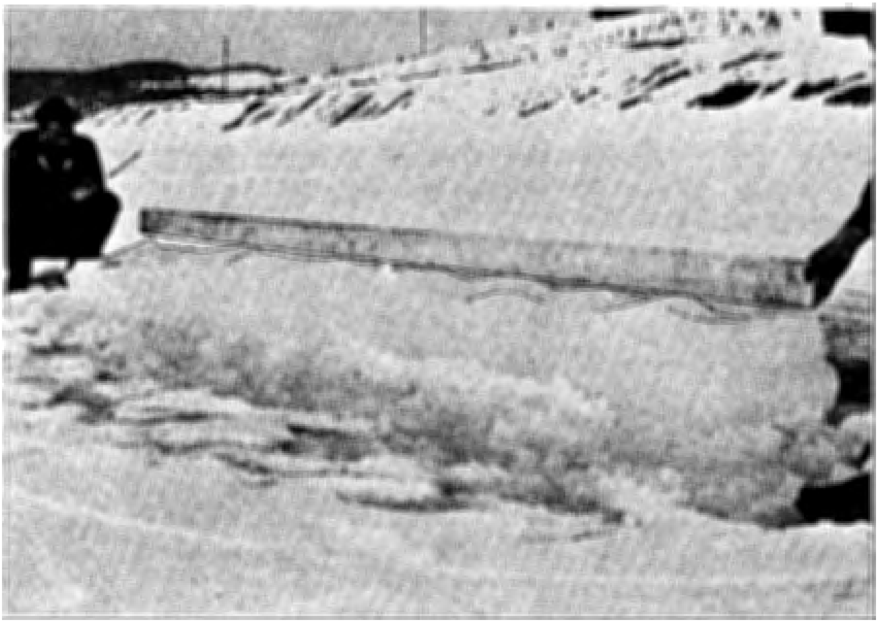

Fig. 5 — Ice floes from the Kilforsen Power canal.

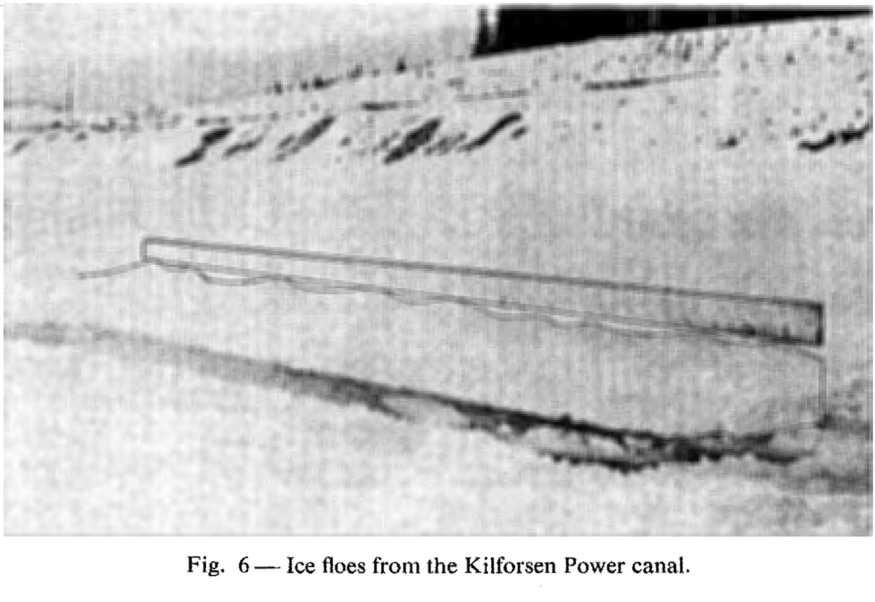

Fig. 6 — Ice floes from the Kilforsen Power canal.

position for 18 days. When turned again, the lower surface shown in Figure 7 had developed a pattern similar to that shown on Figure 2, although the amplitude of the waviness was considerably less. At the same time a new floe was cut and turned, downstream of the above-mentioned. Inspection showed that the surface configuration was similar to that observed 18 days earlier at the upstream floe. During the 18 days the air temperature was low with night temperatures of $-20°C$ and day temperatures from -7 to $-10°C$.

It is commonly assumed that ice with uneven thickness will rapidly become smooth. This is explained in the following way:

At locations with thin ice, the heat transfer would occur at a more rapid rate than at locations with thicker ice, thus resulting in a faster increase of the ice thickness in thin areas than in thick. This is assuming that the air temperature is below the freezing point. Figures 1 to 7 show that this theory does not hold. It appears that any attempt to mathematically describe the heat balance and ice production has to take into account some dynamic properties of the water flow. In connection with this, it is of interest to note the similarity between Figure 7 and Figure 8 which shows "ripples" produced by wind-transported snow. The resemblance to the waviness developed in an erodible channel is also apparent. It seems probable that the same mechanism is responsible for these different phenomena, a mechanism that is not completely understood. It also appears that experiments with flow under an ice cover could contribute to a better understanding of this property of turbulent flow.

Field observations have shown that the ice boundary is not a hydraulically smooth surface. With this in mind, the next step is to evaluate the hydraulic influence of the ice cover.

Hydraulic characteristics of an ice covered channel

From a hydraulic point of view, the ice covering of an open channel causes a radical change of conditions. The ice cover produces a substantial increase of the wetted perimeter, see Figure 9. For a wide channel the hydraulic radius is reduced to near half the value of the open channel radius, assuming a thin cover. The open channel is thus changed to a closed conduit but with the important difference that the cross sectional area will adjust according to the need because the ice is floating on the water surface.

To illustrate the effect of the reduction of the hydraulic radius, assume that the ice roughness is equal to the bottom roughness. If the thickness of the ice cover is assumed to be small, the hydraulic radius is reduced by a

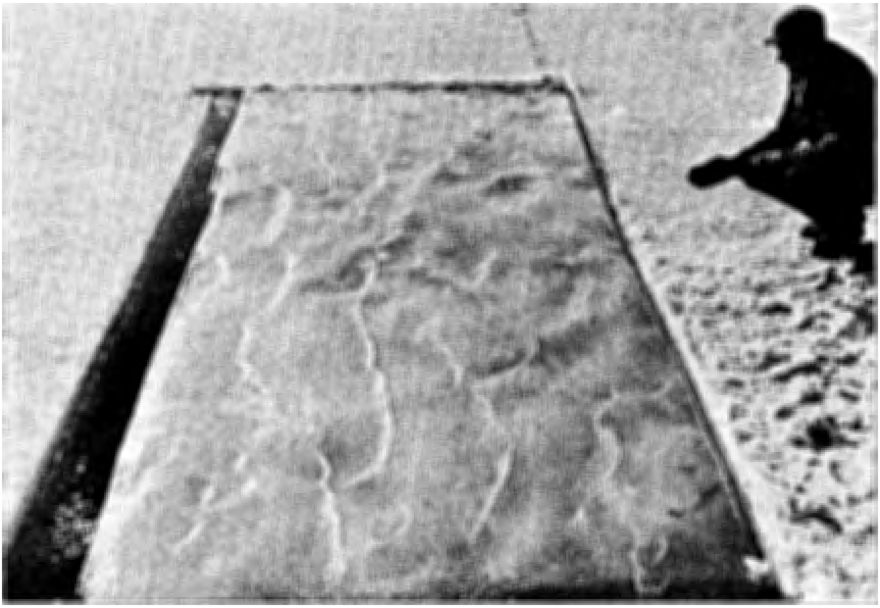

Fig. 7 — An originally smooth ice surface exposed to flow for 18 days.

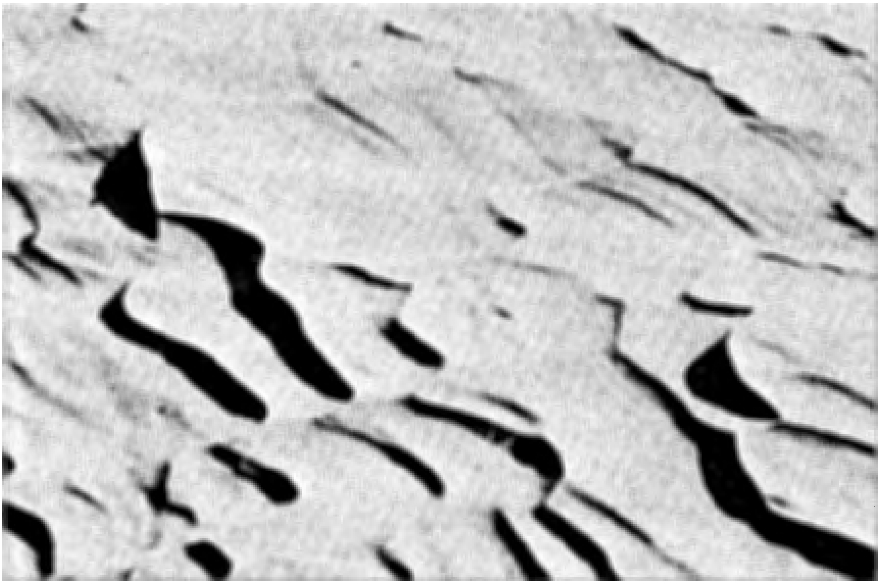

Fig. 8 — Wind-blown snow.

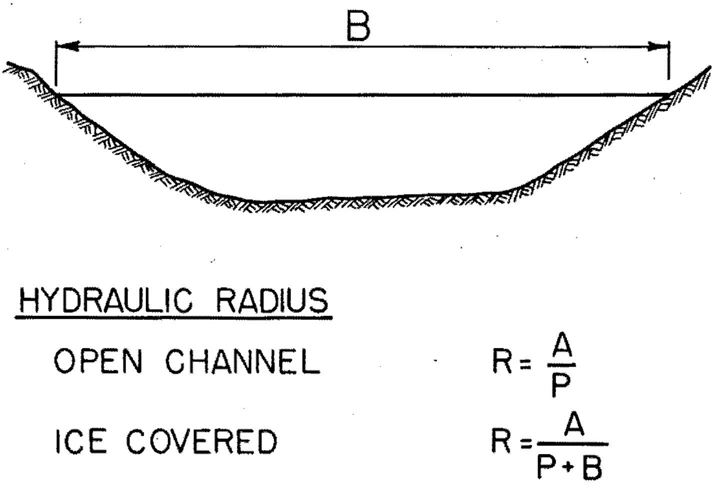

Fig. 9 — Hydraulic radius for open — and ice covered cross section.

factor 2; and if the flow is kept constant, the head loss computed by the Manning equation is 2.5 times the head loss of the open channel.

The assumption of the ice roughness being equal to the roughness of the channel bottom is arbitrary and would, in general, not apply. For the usual case of the two boundaries with different roughness characteristics, a computation based on composite roughness would have to be applied to determine the head losses.

Formula for an equivalent roughness factor.

There are numerous formulas for computing the equivalent roughness factor of a cross section for which the roughness varies from part to part of the wetted perimeter. The cross section is divided into arbitrary subareas, according to the roughness prevailing in each part of the wetted perimeter. To derive an equivalent roughness factor applicable to the whole cross section, one of the following assumptions is generally applied:

1. The mean velocity of each of the subareas is equal to the mean velocity of whole cross section.
2. The resistance to flow of the whole cross section is equal to the sum of the resistances of the subareas.
3. The total discharge of the cross section equals the sum of the discharges of the subareas.

The common procedure in these assumptions is the subdivision of the cross sectional area. In order to derive a correct description of the physical behavior, the sub-areas should be chosen so that the flow within each area is governed by the type of roughness characteristic of the wetted perimeter assigned to that area. It is obvious that condition one above can be true only if the roughness is constant along the entire perimeter. Since the velocity distribution, and hence the mean velocity, are functions of the roughness, the mean velocities of areas with different roughnesses must be different. Condition two, however, is physically correct, provided the subdivision is correct. Condition three is true regardless of the subdivision because it involves only the continuity principle.

A formula which does not suffer any of the shortcomings mentioned, can be derived from the equations for velocity distribution in combination with the continuity equation. In the following derivation, the Manning formula is used for computing the energy loss. It is assumed that the relationship between the roughness height k and the Manning roughness coefficient can be expressed as:

$$n = ck^{1/6} \tag{1}$$

where c = 0.0316 according to C.F. Colebrook.[3] For laboratory use the derivation could as well be based on the Darcy-Weisbach friction factor f, thus eliminating the approximation involved in the above equation. It is further assumed that the flow is rough turbulent, a necessary condition for the validity of the Manning formula.

Let y_t be the total depth of flow in the ice covered channel, see Figure 10. The roughness heights are k_1 and k_2 for the ice cover and for the channel bottom respectively. The velocity distributions near the boundaries are governed by the roughness and the distance to the boundary according to the Prandtl-Karman velocity distribution law. At a particular distance from the boundaries, a maximum velocity occurs that is common to the two distributions. The shear, viscous as well as apparent, is zero at a horizontal plane through this elevation and thus, for uniform flow, this plane determines the subdivision in areas where the velocity distribution is governed by the ice roughness and the bottom roughness, respectively.

The velocity distribution for the upper region is:

$$v_1 = 2.5\, v_{f1} \ln \frac{30}{k_1} y \tag{2}$$

and for the lower region:

3. Colebrook, C. F.: The Flow of Water in Unlined, Lined and Partly Lined Rock Tunnels, 1958.

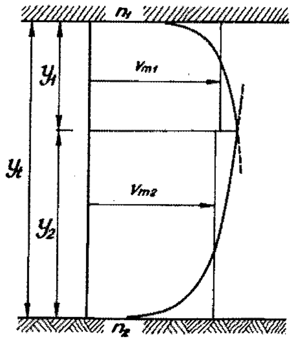

Fig. 10 — Theoretical velocity distribution. Definition sketch.

$$v_2 = 2.5\, v_{f2} \ln \frac{30}{k_2}\, y \tag{3}$$

where y is the distance from the respective boundaries.

The common maximum velocity occurs at the distances y_1 and y_2 from the ice cover and the channel bottom respectively: $(y_1 + y_2 = y_t)$.

$$v_{max} = 2.5\, v_{f1} \ln \frac{30}{k_1}\, y_1 = 2.5\, v_{f2} \ln \frac{30}{k_2}\, y_2$$

hence

$$\frac{v_{f1}}{v_{f2}} = \sqrt{\frac{\tau_1}{\tau_2}} = \frac{\ln \frac{30}{k_2}\, y_2}{\ln \frac{30}{k_1}\, y_1} = \frac{a}{b} \tag{4}$$

where the numerator is set equal to a and the denominator to b.

The mean velocities v_{m_1} and v_{m_2} are obtained by integration of the velocity functions and dividing by y_1 and y_2 respectively. The theoretical velocity is considered to be zero at the distance $\frac{k}{30}$ from the boundaries. The mean velocity for the upper region is:

$$v_{m1} = \frac{1}{y_1} 2.5\, v_{f1} \int_{\frac{k_1}{30}}^{y_1} \ln \frac{30}{k_1} y \, dy = \frac{1}{y_1} 2.5\, v_{f1} \left[y_1 \ln \frac{30}{k_1} y_1 - y_1 + \frac{k_1}{30} \right]$$

or

$$v_{m1} \cong 2.5\, v_{f1} \left(\ln \frac{30}{k_1} y_1 - 1 \right) \tag{5}$$

The term $\frac{1}{y_1}\ 25\, v_{f1} \frac{k_1}{30}$ is generally less than $10^{-3}\, v_m$ and is therefore considered to be negligible.

In the same manner, the mean velocity for the lower region is found:

$$v_{m2} \cong 2.5\, v_{f2} \left(\ln \frac{30}{k_2} y_2 - 1 \right) \tag{6}$$

Division of (5) by (6) and comparison with (4) yields:

$$\frac{v_{f1}}{v_{f2}} = \sqrt{\frac{\tau_1}{\tau_2}} = \frac{v_{m1}}{v_{m2}} \frac{\ln \frac{30}{k_2} y_2 - 1}{\ln \frac{30}{k_1} y_1 - 1} = \frac{v_{m1}}{v_{m2}} \left(\frac{a-1}{b-1} \right) \tag{7}$$

From the assumption of uniform flow it follows that the energy lines of the upper and the lower regions are parallel and also parallel to the energy line of the entire flow, i.e. $S_1 = S_2 = S$

The Manning formula applied to the upper and lower regions and to the whole cross section is:

$$v_{m1} = \frac{1.49}{n_1} y_1^{2/3} S^{1/2} \tag{8}$$

$$v_{m2} = \frac{1.49}{n_2} y_2^{2/3} S^{1/2} \tag{9}$$

$$v_m = \frac{1.49}{n} \left(y_{t/2} \right)^{2/3} S^{1/2} \tag{10}$$

Dividing (8) by (9) yields

$$\frac{v_{m1}}{v_{m2}} = \frac{n_2}{n_1}\left(\frac{y_1}{y_2}\right)^{2/3} \tag{11}$$

(11) combined with (7) and (4) gives:

$$\frac{y_1}{y_2} = \left(\frac{a\,(b-1)}{b\,(a-1)}\,\frac{n_1}{n_2}\right)^{3/2} \tag{12}$$

Finally, when the continuity equation,

$$y_1\,v_{m1} + y_2\,v_{m2} = y_t\,v_m \tag{13}$$

is combined with equations (8), (9) and (10) the following formula for the equivalent Manning coefficient is obtained:

$$\frac{1}{n} = \frac{\frac{1}{n_1}\,y_1^{5/3} + \frac{1}{n_2}\,y_2^{5/3}}{\left(\frac{1}{2}\right)^{2/3}\,y_t^{5/3}} \tag{14}$$

(When the metric system is used, M can be substituted for $\frac{1}{n}$)

This derivation was based on the assumption of a wide channel section where the influence of the side slopes is neglected. This assumption has not been introduced. It is, therefore, of interest to examine the equations further with respect to changes in depth. First, it is noted that the expression for the equivalent Manning coefficient can be written

$$\frac{1}{n} = \frac{(y_1/y_2)^{5/3}\,\frac{1}{n_1} + \frac{1}{n_2}}{\left(\frac{1}{2}\right)^{2/3}\,(y_1/y_2 + 1)^{5/3}} \tag{15}$$

which indicates, that $\frac{1}{n}$ is a function only of the ratio of y_1 to y_2 and thus independent of the total depth y_t . Next it is of interest to investigate the ratio $\frac{y_1}{y_2}$ with respect to y_t . Here it turns out that $\frac{y_1}{y_2}$ varies but slightly with the magnitude of y_t for the practical range of values of n_1 and n_2 . This is very important because it implies that it is possible to definitely compute the equivalent roughness factor for any given set of roughness coefficients n_1 and n_2 and thus to present a complete solution to the problem as a dimensionless plot. Figure 11 gives the ratio $\frac{n}{n_2}$ as a function of $\frac{n1}{n_2}$ in the range

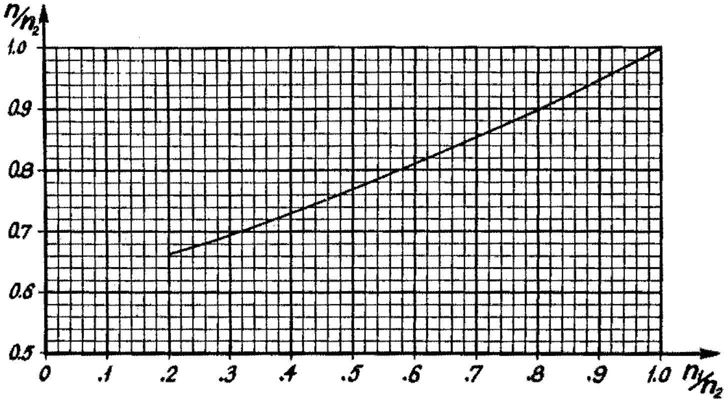

Valid for $n_2 \leq 0.04$ and $y_t \geq 5$ feet with an accuracy of 1% or better. Jncreasing accuracy with increasing total depth y_t.

Fig. 11 — Composite roughness as a function of ice — and bottom roughness.

from 0.2 to 1.0, assuming $n_2 \leqq 0.04$ and $y_t \geqq 5$ feet. Here n_1 is the Manning n for the smoother of the two boundaries involved. Therefore the curve is valid also for the case where the ice roughness is greater than that of the channel bottom. In this case, obviously, the subscripts have to be interchanged.

It would appear that the expression for the equivalent roughness factor is valid for any cross sectional shape. This is, however, not true because the Prandtl-Karman law gives the velocity at a given point and for a given flow as a function of the wall roughness and the perpendicular distance from the point to the wall. Therefore, when a sloping portion of the cross section is considered, the distance to the plane of zero shear should be measured perpendicular to the slope.

If the total depth at a particular point is $y_t = y_1 + y_2$, the ratio of the distances determining the plane of zero shear is $\frac{y_1}{y_2 \cos \alpha}$ where α is the slope angle, see Figure 12. The error committed thus increases with the cosine of the angle, but for flat slopes is of minor importance.

With the composite Manning coefficient being determined according to the method indicated, head loss computations for the ice covered channel can be performed in the ordinary manner. The hydraulic radius is computed from $A/(P + B)$ where B is the width of the underside of the ice

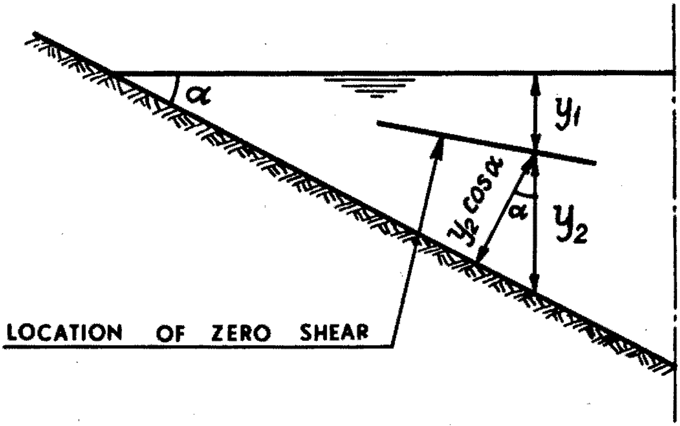

Fig. 12 — The effect of channel side slope. Definition sketch.

cover, and the cross sectional area A is corrected for the portion occupied by ice if the ice thickness is appreciable.

Determination of roughness from measured velocity distribution.

If the Prandtl-Karman equation for fully developed turbulence is assumed to be valid, the roughness of the boundary can be determined when the velocity distribution is known. Let y_0 be an arbitrary distance from the boundary. Equation (5) yields for the mean velocity:

$$v_m = 2.5\, v_f \left(\ln \frac{30}{k} y_0 - 1 \right) \tag{16}$$

The velocity at the distance y_0 from the boundary is determined from equation (2):

$$v_{max} = 2.5\, v_f \ln \frac{30}{k}\, y_0 = 2.5\, v_f\, a_1 \tag{17}$$

Division of equation (16) by equation (17) yields:

$$\frac{v_m}{v_{max}} = \frac{a_1 - 1}{a_1}$$

or

$$a_1 = \ln \frac{30}{k}\, y_0 = \frac{v_{max}}{v_{max} - v_m} = \frac{1}{1 - \dfrac{v_m}{v_{max}}}$$

from which $$k = 30\, y_0\, e^{-a_1} \tag{18}$$

The measured velocity distribution is plotted and the depth y_0 is chosen so that an accurate determination of a_1 is obtained. The mean velocity is determined and the roughness height then computed from equation (18). The Manning coefficient is finally computed from equation (1).

Determination of the roughness height can also be performed graphically by plotting the measured velocities on semilogarithmic paper where the measured velocities should fall on a straight line. This gives a convenient procedure for smoothing the measured values. The roughness height k is then found from the slope of the straight line as follows:

$$k = 30\, y^1 = 30 \times 10^{-\frac{v_{1.0}}{v_{1.0} - v_{0.1}}} \tag{19}$$

y^1 is the value of y for which the straight line intersects the velocity axis. $v_{1.0}$ and $v_{0.1}$ are the velocities at the distances 1.0 and 0.1 from the boundary, respectively.

Field Measurements

In order to obtain some information about actual ice roughness and about the increase of head losses due to an ice cover, a comprehensive field investigation was planned and performed by the Swedish State Power Board in 1960. The measurements were planned to be carried out on two occasions, one in summertime when the channel was open, and one in the wintertime with an ice cover on the channel. It was anticipated that the open channel measurements would give the roughness of the channel bottom, and the winter measurements would give the combined effect of ice roughness and the known bottom roughness. In addition, a comprehensive investigation of the velocity distribution close to the ice cover would yield information on the ice roughness.

The measurements were made in the supply channel of the Kilforsen Power Plant. Figure 13 gives a plan of the waterways adjacent to the power station. The water enters the head race from a pond approximately 17 miles long formed by damming the river Fjällsjöälven. The head race consists of a 6000-foot open channel, a 12,000-foot free-surface tunnel and a 2600-foot forebay. The station utilizes a head of close to 330 feet and discharges through a full-flowing tunnel about 9000 feet long. With a maximum flow of 13,200 cfs, the capacity is 340 MW from three units. As seen from the

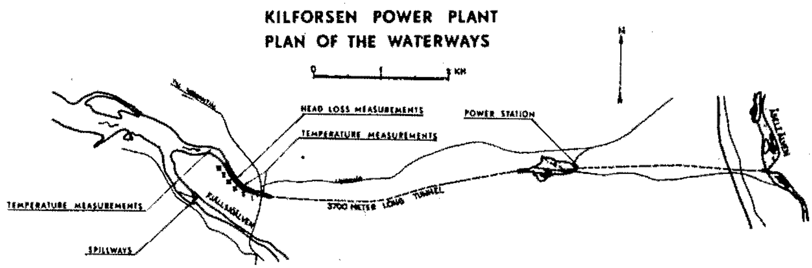

Fig. 13 — Plan of the Kilforsen Hydro Power Plant.

figures given, the plant is well adapted for the purpose of frequency and peak demand regulation which is generally performed by this station in coordination with other similar stations.

For the actual tests it was essential that the flow be kept constant during each test period. Therefore, the turbines were locked at a constant output during each run. The discharge was determined from the output, the over-all efficiency being known from recently-performed efficiency tests.

The winter measurements were carried out from February 23 to 26, 1960. The ice, at that time approximately 2 months old, was between 2 and 3 feet thick close to the channel banks, while the thickness on the main part of the channel varied between 4 and 8 inches.

A 2300-foot long section of the supply channel was chosen for the measurements, see Figure 14. Holes were drilled through the ice in six locations along this section, and steel poles were driven into the channel bottom. The elevation of the tops of the poles was determined by accurate leveling.

The velocity distribution was measured in four cross sections, see Figure 14. Holes were cut in these sections for insertion of the current meters. The meters had long tail fins and were suspended by wires because of the great depths. The holes, three feet long and 6 inches wide, were cut with the long direction perpendicular to the flow. Figure 15 shows examples of the velocity measurements, the crosses indicating the position of measuring points.

The velocity measurements were carried out by one crew at each cross section, and determined the duration of each test run. The time required was of the order of 3 hours, during which time the water surface elevation was measured every 5 minutes. The 2-to 3-foot deep holes served as stilling wells to produce a calm water surface, the elevation of which was measured with a ruler (1 mm divisions) from the top of the poles. The head between

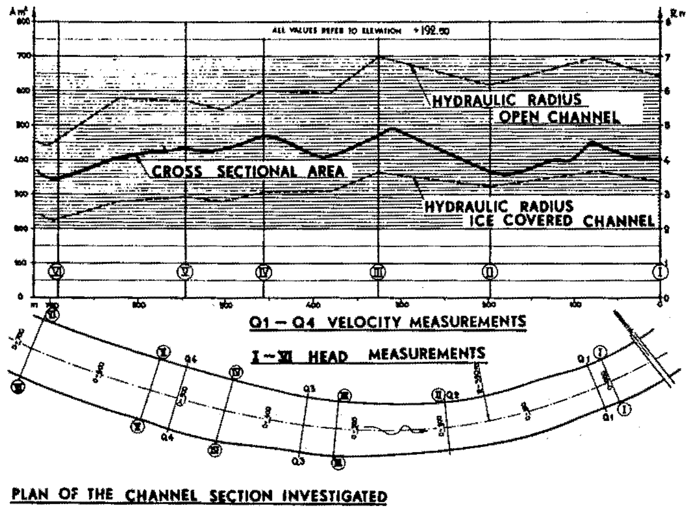

Fig. 14 — Plan of the investigated part of the power canal. Variation of cross sectional area and hydraulic radius.

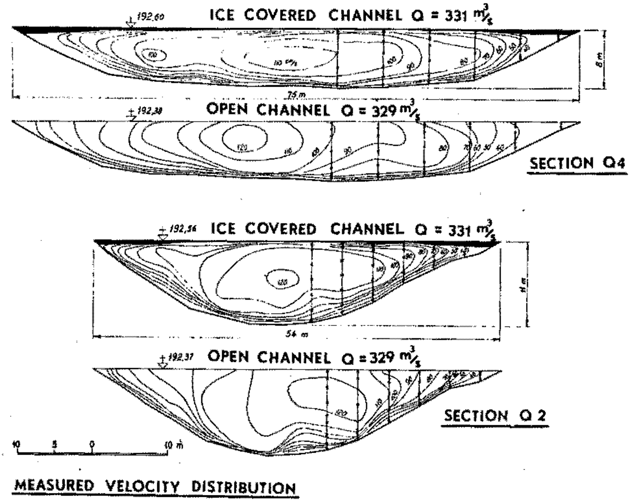

Fig. 15 — Velocity distribution in two cross sections. With and without ice.

the forebay and the draft tube exit, and the power output also, were measured every 5 minutes during each test. Measurements were performed with 4 different discharges in the range from 6100 cfs to 11,800 cfs.

The summer measurements, June 16-20, 1960, were performed in a similar way. Due to the smaller losses to be expected, a higher degree of accuracy was required. Accordingly, the water surface elevation was determined using point gages (1/10 mm reading) placed in stilling wells. The relative elevation of the point gages was established by hydrostatic leveling.

Velocity distribution was measured in two cross sections and at 4 different flows. Head losses were determined at 9 flows in the range from 5300 cfs to 12,400 cfs.

Wind velocities ranged between 0 and 9 fps, mainly in the direction of the channel flow, but did not affect the accuracy of the measurements.

During both summer and winter measurements, the flows into the Kilforsen reservoir were regulated to maintain the test flows in order to minimize variations in reservoir and channel surface elevation. Sufficient time was allowed prior to each test to reach a steady state condition.

During the summer measurements the channel reach was sounded at 9 cross sections. Since it was found that the cross sectional area was rather variable, see Figure 14, complementary soundings were made later. Thirty-eight new cross sections were introduced reducing the distance between successive cross sections to 65 feet. Figure 16 shows 6 typical cross sections.

Treatment of the Data Collected

The data obtained from the field measurements consisted of water surface elevations at six sections along the channel, at the power station intakes, and at the draft tubes, and of power output from the plant. The head losses in the supply tunnel were also measured to determine the roughness of the tunnel.[4] All of the data mentioned were time correlated. The water surface elevations were plotted as functions of time for each flow rate investigated. For each test period, a time interval was chosen within which the fluctuation of the surface elevations showed a minimum, and the average elevation was determined for this interval. This was done for each of the above-mentioned sections. Thus the result was an accurate water surface profile for each flow, and an accurate head at the power station. Accuracy determination based on the gathered data indicated a standard deviation of

4. See ASCE, Journal of the Hydraulics Division, HY4, July 1966: Factors Influencing Flow in Large Conduits, discussion by S. Angelin and Peter Larsen.

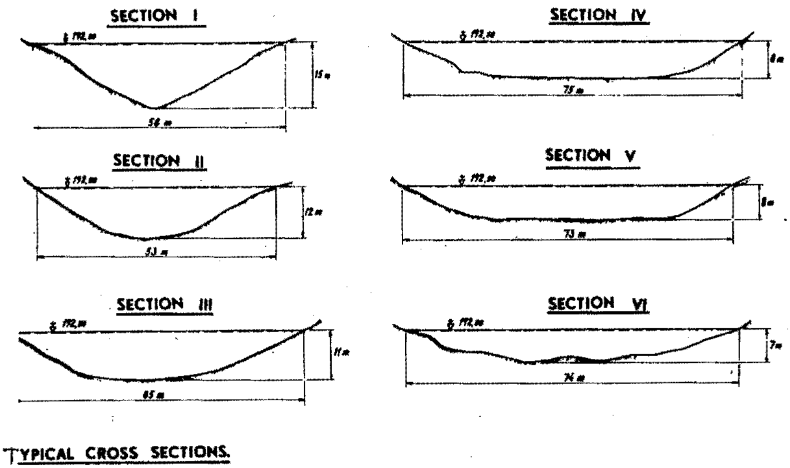

Fig. 16 — Typical cross sections.

0.7 and 0.5 mm in the water surface elevation of a section, for the winter and summer conditions respectively. The standard deviation for the difference in elevation of the water surface at the ends of the 2300-foot test reach was found to be 2.2 mm and 0.5 mm for the winter and summer conditions respectively.

The flow rate determined from the power output and the measured head were believed to run within 1% of the actual value for all tests.

The water surface profiles obtained for various flow rates were used, together with the soundings from 38 cross sections, as a basis for backwater computations. Since the Manning "n" was the unknown, it was varied in order to obtain the best agreement between measured and computed water surface profiles.

To obtain a comparison between the head losses for the open channel and those for the ice covered channel, all measurement results had to be converted to a common stage. Since the differences in stages at different tests were small ($\pm$ 0.7 feet from the chosen reference stage), the corrections needed to take into account only changes in cross sectional area, the changes in wetted perimeter being insignificant.

The velocity distribution measurements were treated according to the theoretical approach. Figure 17 shows the velocity distribution on a vertical measured at 4 diferent flows, and the computations based on these data. This was done for 40 verticals yielding 160 determined k values, the average of which was used for computation of the Manning "n" according to equation (1).

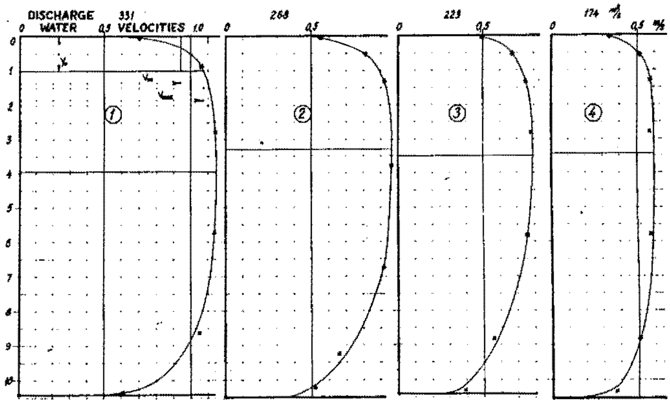

	y_o (m)	V_{max} (m/s)	V_m (m/s)	a	k (m)	M ($m^{1/3}/s$)	Q (m^3/s)
①	1,00	1,075	0,945	8,20	$8{,}26 \cdot 10^{-3}$	57,8	331
②	1,00	0,887	0,776	8,00	$10{,}1 \cdot 10^{-3}$	55,9	268
③	1,00	0,727	0,639	8,20	$8{,}26 \cdot 10^{-3}$	57,8	223
④	1,00	0,544	0,477	[illegible]	$8{,}94 \cdot 10^{-3}$	56,9	174

$a = \frac{1}{1 - \frac{V_m}{V_{max}}}$; $k = 30 y_o e^{-a}$; $M = \frac{26}{\sqrt[6]{k}}$

ROUGHNESS DETERMINATION FROM MEASURED VELOCITY DISTRIBUTION

Fig. 17 — Vertical velocity distribution with 4 different flow rates.

Measurement Results

The results of the measurements made it possible to compare the composite roughness of the channel obtained in two different ways. The head loss computations gave n = 0.0333 for the open channel. This value of the Manning coefficient fitted all measured surface profiles equally well. An example of the measured and computed water surface profiles is given in Figure 18.

For the ice covered channel, it was similarly found from the head loss computations that n = 0.0270. Figure 19 shows an example of measured and computed surface profiles for the ice covered channel. Based on accuracy estimates it was concluded that:

Manning coefficient for the open channel, n = 0.0333 ± 0.0003

Manning coefficient for the composite roughness, n = 0.0270 ± 0.0007

The roughness of the ice cover was determined from the measured velocity distribution close to the cover. It was found that the Manning coefficient for the ice cover, n = 0.0192. Entering the Manning n-values, found for the channel bottom and for the ice cover, into the formulas for composite roughness, or using the diagram Figure 11, it was found that the Manning coefficient for the composite roughness n = 0.0267.

This result compared closely with the value determined by direct measurements.

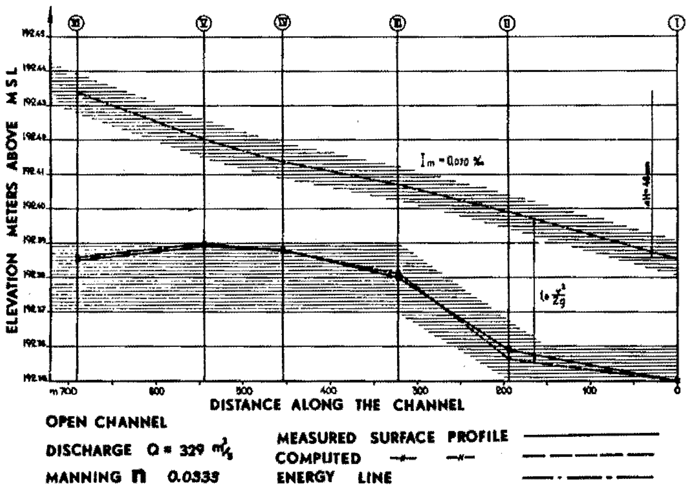

Fig. 18 — Computed and measured water surface profile without ice.

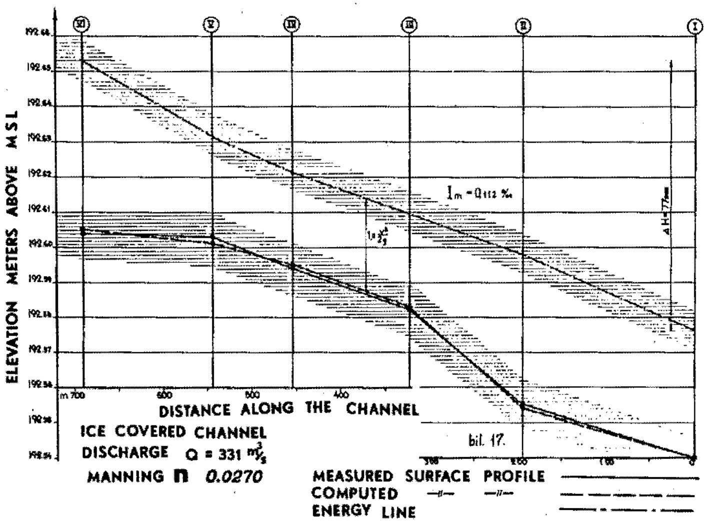

Fig. 19 — Computed and measured water surface profile with an ice cover.

The Manning coefficient for the open channel is high. This can be explained by the fact that the major part of the channel reach investigated is lined with a loose rip-rap protection consisting of bed rock material from the blasted supply tunnel.

It should be noted that the values of roughness height, computed primarily from the plotted velocity profiles, showed rather great fluctuations. This would, to some degree, be expected because the roughness varies from place to place, as seen from the photographs, Figures 1 to 6.

The head losses, referred to a common stage, are shown on Figure 20. The head losses with the ice cover was found to be 62% greater than the head losses of the open channel. It should be noted, however, that the channel investigated was rather rough, and that the head losses due to an ice cover could therefore be expected to amount to higher percentages of the open channel losses than those indicated above.

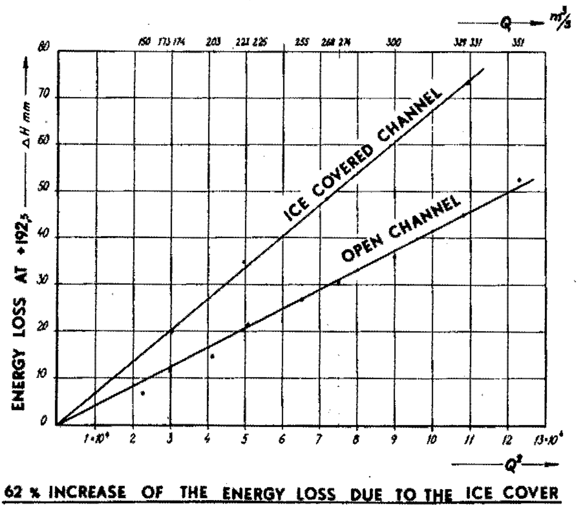

Fig. 20 — Head losses with and without an ice cover related to a common stage.

Concluding Remarks

The under surface of ice on a channel has been found to have irregularities that are formed by the flowing water. The effect of these irregularities corresponds to a certain roughness expressible in terms of an equivalent roughness height. The mechanics of the formation, however, are not known, and therefore it is not possible at the present time to predict the roughness of the ice cover on a channel of given hydraulic characteristics and given climatic conditions. Two lines of approach should be followed in order to adequately investigate the phenomena involved. The gathering of field data should continue, but this should be supplemented by systematic research and laboratory studies.

The formula derived for composite roughness is based on the assumption of two parallel (or slightly converging) boundaries, an assumption which merely limits the applicability to the case considered in this paper. The approach to the problem indicated herein, may be applicable to an attempt to develop a more general solution to the problem of composite roughness. The need for such a solution is obvious, both for design purposes and for laboratory use. Typical design problems include partly lined tunnels and channels with different construction materials used for bottom and side wall. A most significant example in the laboratory is in connection with flume tests conducted to evaluate the properties of various types of roughness. Numerous tests of this type have been performed in either relatively wide flumes, where the effect of the side walls has been disregarded, or in approximately square-shaped flumes with smooth sidewalls, the influence of which has been evaluated by some of the common formulas.

PROCEEDINGS OF THE SOCIETY

Minutes of Meeting

Boston Society of Civil Engineers

November 13, 1968.—A Joint Meeting of the Main Society with the Structural and Construction Sections was held at Nick's Restaurant, 100 Warrenton Street, Boston Mass. Following a dinner preceeding the meeting President Harl P. Aldrich, Jr., called the meeting to order at 7:00 P.M.

President Aldrich stated that the Minutes of the meeting held October 16, 1968 would be published in a forthcoming issue of the Journal and that the reading of those minutes would be waived unless there was an objection. There was none.

President Aldrich announced the death of the following members:—

> Thomas A. Appleton, elected a member April 21, 1916, who died in April, 1968.
>
> Timothy F. Creedon, elected a member March 17, 1937, who died in 1967.
>
> Elson T. Killam, elected a member June 20, 1950, who died May 27, 1968.
>
> Lawrence G. Ropes, elected a member March 21, 1923, who died June 25, 1968.

As there was no other business from the floor President Aldrich turned the meeting over to Arthur H. Mosher, Chairman of the Construction Section to conduct any business of that Section at this time. Mr. Mosher in turn turned the meeting over to Albert B. Rich, Chairman of the Structural Section to conduct any business of that Section at this time.

Chairman Rich introduced the guest speakers of the evening Mr. Charles A. Richardson and Mr. Morse H. Klubock of Perini Corporation and Mr. Zoltan A. Stacho of Parsons, Brinckerhoff, Quade & Douglas, who presented an illustrated talk on "M.B.T.A. Tunnel — Haymarket Square to Charlestown — Design and Construction".

A question period followed the talk.

Ninety-five members and guests attended the dinner and meeting.

Respectfully submitted,

Paul A. Dunkerley
Secretary pro-tem

December 4, 1968.—A Joint Meeting of the Boston Society of Civil Engineers with the Sanitary Section was held in the Society Rooms, 47 Winter Street, Boston, Mass. The meeting was called to order at 7:00 P.M., by President Harl P. Aldrich following an informal dinner at the Mayflower Coffee House and Pub Plaza at One Center Plaza, Boston, Mass.

President Aldrich stated that the Minutes of the meeting held November 13, 1968 would be published in a forthcoming issue of the Journal and that the reading of those minutes would be waived unless there was an objection. There was none.

The Secretary read a list of fifty-four names of those who have applied for membership.

President Aldrich commented on the excellent efforts of the Membership Committee under the leadership of Max Sorota, Chairman.

Necrology — President Aldrich asked for a standing moment of silence in tribute to those who have been lost to us by death since our last meeting as follows:—

> James M. Driscoll, who was elected a member May 20, 1914, who died November 11, 1968.
>
> James P. Kelley, who was elected a member December 15, 1952, who died November 11, 1968.

Since there was no other business from

the floor President Aldrich turned the meeting over to Charles A. Parthum, Chairman of the Sanitary Section to conduct any section business.

Chairman Parthum introduced the guest speaker of the evening, Mr. Ariel A. Thomas, Senior Vice President, Metcalf & Eddy.

Mr. Thomas described a nine year old waste water treatment plant now serving the Pittsburgh, Penn., area. He described the features of the plant and indicated that the existing unit would become a primary treatment plant when a new secondary treatment plant is added. The addition will be required because of an upgrading of specifications for the effluent. The talk was illustrated and Mr. Thomas explained each feature of the addition, how it would function, and the expected product. It is expected that this paper will be published in a forthcoming issue of the Journal.

A question period followed the talk.

About forty members and guests attended the meeting.

Respectfully submitted,

Paul A. Dunkerley
Secretary

January 22, 1969.—A Joint Meeting of the Main Society with the Hydraulics Section was held in the United Community Services Building, 14 Somerset Street, Boston, Mass. Following the dinner at which 75 members and guests were present, President Harl P. Aldrich, Jr., called the meeting to order at 7:00 P.M.

President Aldrich stated that the Minutes of the meeting held on December 4, 1968 would be published in a forthcoming issue of the Journal, and that the reading of those Minutes would be waived unless there was an objection. There was none.

President Aldrich called upon the Secretary who read a list of forty-seven names of those whose applications for membership had been received.

The Secretary presented a recommendation from the Board of Government for action by the Society at this meeting, as follows:—

> MOTION "to recommend to the Society that the Board of Government be authorized to transfer an amount not to exceed \$4000.00 from the Principal of the Permanent Fund to the Current Fund for Current Expenditures".
>
> It was VOTED "that the Board of Government be authorized to transfer \$4000.00 from the Principal of the Permanent Fund to the Current Fund".

President Aldrich stated that this was the first of two votes required, and that the second and final vote would be taken at the monthly meeting in February.

President Aldrich announced that this was a joint meeting with the Hydraulics Section and yielded the rostrum to Mr. A. A. Vulgaropulos to conduct the business of that Section.

President Aldrich declared a brief recess while the furniture was rearranged.

President Aldrich announced that this meeting was sponsored by the John R. Freeman Fund Committee as a John R. Freeman Memorial Lecture. Because of illness, Past President Leslie J. Hooper, Chairman of the John R. Freeman Fund Committee was unable to be present. Vice President Robert H. Culver introduced the speaker of the evening, Mr. Thomas R. Camp.

The subject of Mr. Camp's paper was "Hydraulics of Mixing Tanks". Mr. Camp used two slide projectors to explain the highlights of his very interesting paper. It is to be expected that the paper will be published in a forthcoming issue of the Journal. At the conclusion of the talk an interesting question period followed.

Eighty-eight members and guests attended the business meeting and the lecture.

The meeting adjourned at 8:30 P.M.

Respectfully submitted,

Paul A. Dunkerley
Secretary

SANITARY SECTION

December 4, 1968.—President Aldrich opened the joint meeting with Main Society in the Society Rooms at 7:00 P.M. After conducting certain Society Business including the reading (by Secretary Paul Dunkerley) of the names of fifty new members, the meeting was turned over to the Sanitary Section Chairman, Charles A. Parthum.

A nominating committee consisting of Mr. William Traquair, Professor Robert Meserve and Mr. Walter Newman, Chairman, was appointed to submit a slate of officers for the coming year at the March 5, 1968, Annual Section Meeting.

Chairman Parthum then introduced the speaker of the evening, Mr. Ariel A. Thomas, Senior Vice President of Metcalf & Eddy, Inc. who presented a paper on the "Design of the 150 MGD Secondary Treatment Facilities for the Allegheney County Sanitary District. The presentation was illustrated with slides and traced the development of the plant through the primary treatment units and the new secondary facilities. An interesting question and answer period followed.

Attendance was about 40 and the meeting was adjourned at 8:30 P.M.

Charles A. Parthum for
Leland Charter, Clerk

HYDRAULICS SECTION

November 6, 1968:—A meeting of the Hydraulics Section of the Boston Society of Civil Engineers was held in the Society Rooms, 47 Winter Street, Boston, Massachusetts. The meeting was called to order at 6:40 P.M. by Mr. Athanasios A. Vulgaropulos, Chairman of the Section. Mr. Vulgaropulos reported on the general results of the Questionnaire which had been circulated to all members of the Society. Mr. Vulgaropulos also reported on the Section's field trip of October 5, 1968 to the Hurricane Barriers constructed by the U.S. Corps. of Engineers in Providence, Rhode Island and New Bedford, Massachusetts. Notices of future meetings of this Section and of other sections of the Society were read.

The Chairman then presented the format for the evening's workshop and introduced the various panel speakers and their topics, who were as follows:

Research: Murray B. McPherson, Director, Urban Water Resources Research Program of the American Society of Civil Engineers at Harvard University.

Climatology and Hydrology: Robert E. Lautzenheiser, Meteorologist in Charge, U.S. Weather Bureau Office for State Climatology, Boston, Mass.

Administration and Financing: Willard S. Pratt, Director, Department of Public Works, City of Newton, Mass.

Planning and Design: Charles Fuller, Project Engineer, Camp, Dresser & McKee, Consulting Engineers, Boston, Mass.

Design Criteria and Design: Robert A. Carleo, Project Manager of Water Resources, Howard, Needles, Tammen & Bergendoff, Consulting Engineers, Boston.

Construction: Carl Buccella, R. A. Buccella & Son, Inc., Contractors, Avon, Mass.

Many questions followed these presentations, however, due to the hour, question time was curtailed.

The meeting had an attendance of 40 and was adjourned at 9:15 P.M.

Respectfully submitted,

Stephen E. Dore, Jr.
Clerk

January 22, 1969:—The Annual Meeting of the Hydraulics Section was held jointly with the Main Society of the Boston Society of Civil Engineers in the Adams Room of the United Community Services Building, 14 Somerset Street, Boston, Mass. The meeting was opened by President Harl Aldrich of the Society at 7:00 P.M. President Aldrich called on Treasurer Paul A. Dunkerly to read a list of new applicants for admission. President Aldrich then turned the meeting over to Mr. Athanasios A. Vulgaropulos, Chairman of the Hydraulics Section, to conduct the business of the Section. Chairman Vugaropulos read the report of the Nominating Committee, consisting of Nicholas Lally, Peter S. Eagleson and Allan Grieve, Jr., who presented the following slate of Officers for the Hydraulics Section to serve during the year 1969-1970; who were subsequently elected by voice vote:

Chairman, Ronald T. McLaughlin
Vice-Chairman, Stephen E. Dore, Jr.
Clerk, Albert G. Ferron
Executive Committee, Jerome Degen, Frank E. Perkins, Robert S. Restall

Upon conclusion of the Section business Chairman Vulgaropulos turned the meeting back to President Aldrich, who in turn called on Dr. Robert Culver, first Vice President of the Society, to introduce the speaker of the evening. Dr. Culver presented Mr. Thomas R. Camp, Consulting Engineer, who delivered the fourth John R. Freeman Memorial Lecture speaking on "Hydraulics of Mixing Tanks".

Mr. Camp discussed the mixing of liquids as widely used in chemical, pharmaceutical and food industries and in water and wastewater treatment to disperse additives, homogenize two or more liquids and for flocculation. The paper analyzes rotary mixing in terms of energy dissipation by internal shear, and introduces design procedures in terms of the drag on the rotors, stators and tank walls.

After a brief questions and answer period, President Aldrich presented to Mr. Camp a certificate for the lecture and a check in behalf of the John R. Freeman Memorial Fund. The meeting was adjourned at 8:40 P.M. Attendance at the dinner preceeding the meeting was 75 and attendance at the meeting was 88.

Respectfully submitted,

Stephen E. Dore, Jr.
Clerk of the Hydraulics Section

TRANSPORTATION SECTION

November 20, 1968:—A luncheon meeting of Boston Society of Civil Engineers, Transportation Section, was held on Wednesday, November 20, 1968. After luncheon, the meeting was opened, with 49 members present, by Chairman Maurice Freedman at 12:45 P.M.

Minutes of previous meeting were read and accepted. Mr. Freedman then introduced the guest speaker, Mr. A. S. Plotkin, Transportation Editor of the Boston Globe, who gave his concept of the 'Social Impact of Urban Highway Location'. His very informative and knowledgeable presentation was followed by a question and answer period.

The meeting was adjourned at approximately 1:25 P.M.

Respectfully submitted,

A. Paul LaRosa, Clerk

Abstract of talk by Mr. A. S. Plotkin, Transportation Writer for The Boston Globe, before a meeting of the Transportation Section of the BSCE on November 20, 1968.

THE SOCIOLOGICAL IMPACT OF URBAN HIGHWAY LOCATION

"I have seen the future and it doesn't work." This was the reaction of a New York newspaperman to the problems of the freeway system of a large western city. Urban highway problems cannot be ignored, and were the subject of a recent conference in Washington sponsored by the Highway Research Board. The message it produced is that the nation's road builders must learn how to make highways work for people, not against them.

The consideration of local community values in connection with highways is not a passing whim that will change with government administrations. Many of the complaints associated with the Embarcadero in San Francisco, the present Baltimore project, some of New York's interborough expressways, and the Inner Belt and Southwest Expressway in Metropolitan Boston, are sound and cannot be ignored. Boston need not be ashamed of the efforts that have been made to minimize the adverse impact of these highways, but more may have to be done in cooperation with local neighborhood and community groups.

Broad urban highways have a profound effect on their environs. An embankment can create a "Chinese Wall" effect, while the cost of depressing a highway or rail corridor may be staggering. In Greater Boston we are relatively fortunate in that the Belt route recommended would not have as devastating an effect as would some highways proposed for other cities. In spite of some opinions to the contrary, it is felt that the difficulties can be resolved and the Belt finished by 1975 or 1976. When some sections are settled, there will be strong pressures to resolve the remaining problems.

The idea that a highway can actually improve an urban neighborhood by melding with schools and recreation facilities, model cities developments, shopping plazas and office buildings to bring new property taxes to a city, should not be discarded. However, most desirable schemes will cost money and consequently face delays in getting funds. Nevertheless, the number of automobiles will continue to increase, and this pressure will force action on highway improvements. The answers are anything but simple, and conditions may get worse before they get better.

There is currently agitation for a Massachusetts Department of Transportation which would act something like a holding company for various state agencies. This could be useful. A similar arrangement now operating in New York State could provide some guidelines.

TIBBETTS ENGINEERING CORP.

CIVIL—SANITARY—STRUCTURAL CONSULTING

41 FRONT ST. PIER 9
NEW BEDFORD, MASS. 02740

WESTON & SAMPSON

Sanitary-Civil

Consulting Engineers

Water Supply, Treatment, Distribution
Sewerage, Sewage & Industrial Wastes
Treatment, Supervision of Treatment
Water & Air Pollution Studies—Rates
Drainage Flood Control Refuse Disposal

10 High Street Boston, Mass. 02110

CHARLES R. VELZY ASSOCIATES, INC.

Consulting Engineers

Water Pollution Control —Water Supply
Drainage
Solid Waste Disposal — Industrial Wastes

300 Martine Ave., White Plains, N.Y.
Mineola, N.Y. New City, N.Y.

FRANK H. WHELAN, INC.

Consulting Engineers

Bridges Buildings
Appraisals Investigations

1616 SOLDIERS FIELD ROAD
BOSTON, MASS. 02135
Phone 254-9011

WALK, HAYDEL & ASSOCIATES, INC.

Complete Industrial Plant Design; Process Design; Civil, Chemical, Mechanical, Electrical, Structural, Instrumentation, Materials Handling, Machine Design
Architect—Engineer Services
762 Bayonne St., New Orleans, La., 70113
Phone 504-529-2133

W&H

100 YEARS OF SERVICE

WHITMAN & HOWARD, INC.

ENGINEERS AND ARCHITECTS

89 BROAD STREET, BOSTON, MASS.

JOSEPH S. WARD and ASSOCIATES

CONSULTING ENGINEERS

Engineering Geology **Earthworks**
Soils and Foundations **Reclamation**
Retaining and Waterfront Structures **Pavements**

91 Roseland Avenue,
Caldwell, New Jersey 07006
Telephone: 201-226-9191

WOODWARD-CLYDE & ASSOCIATES

Consulting Engineers and Geologists in Applied Earth Sciences

EXECUTIVE OFFICES
420 MONTGOMERY ST., SAN FRANCISCO
2 Pennsylvania Plaza, New York, N.Y. 10001
Engineering Offices
Oakland, San Jose, Los Angeles, San Diego, Orange, California, Philadelphia, St. Louis, Kansas City, Denver, Clifton, New Jersey

---

E&K **EDWARDS and KELCEY**

Engineers and Consultants

470 Atlantic Ave., Boston, Mass.

GREEN ENGINEERING AFFILIATES

Consulting Engineers

Water Supply and Treatment
Sewage and Industrial Waste Treatment
Storm Drainage Systems and Sanitary Sewers
Highways, Bridges & Structures

625 McGrath Highway
Winter Hill Branch
Boston, Massachusetts
617 623-2311

COMMITTEES 1968 - 1969

NOMINATING COMMITTEE

John F. Flaherty

George G. Bogren
Robert L. Fuller
Robert L. Meserve
Lee Marc G. Wolman
(Term expires March, 1969)

William A. Henderson
Donald T. Goldberg
Charles C. Ladd
Robert J. Van Epps
(Term expires March, 1970)

PROGRAM

Harl P. Aldrich, Jr., *Chairman*

Charles O. Baird, Jr.
Robert H. Culver
Sepp Firnkas
Maurice Freedman
H. Hobart Holly
Arthur H. Mosher
Charles A. Parthum
Albert B. Rich
Ernest L. Spencer
A. A. Vulgaropulos

PUBLICATION

Charles Y. Hitchcock, Jr., *Chairman*

Maurice Freedman
Donald R. F. Harleman
H. Hobart Holly
Arthur H. Mosher
Charles A. Parthum
Steve J. Poulos
Albert B. Rich
A. A. Vulgaropulos

LIBRARY

Harry L. Kinsel, *Chairman*

John M. Biggs
Joseph Capone
George W. Hankinson
William H. Parker, 3rd.
Nathaniel N. Wentworth

HOSPITALITY

Thomas Tsotsi, *Chairman*

Philip Bianchi
William P. Breen
Kenneth M. Childs
Ralph H. Cross, 3rd.
Conrad Fagone
William P. Kramer
Thomas Turton

MEMBERSHIP

Max D. Sorota, *Chairman*

Richard F. Battles
Richard de Neufville
Charles H. Flavin
J. E. Giles, Jr.
Robert L. McGillicuddy
Robert L. McWilliams
Wesley F. Restall
Warren H. Ringer
Edward N. Smith
George K. Tozer
Martin E. Weiss
Gerald L. Woodland, Jr.
Newton L. Worth
John T. Yunits
William Zoino

ADVERTISING

Paul S. Crandall, *Chairman*

Francis T. Bergin
Walter M. Newman
Frank W. Stockwell, Jr.
Robert J. Van Epps

JOINT LEGISLATIVE COMMITTEE

Cornelius J. O'Leary, *Chairman*

James L. Dallas
Joseph Knox
Charles A. Parthum
Ralph M. Soule

PROFESSIONAL CONDUCT

E. Sherman Chase, *Chairman*

Francis S. Harvey
William L. Hyland
George G. Bogren

PUBLIC RELATIONS

Richard F. Battles, *Chairman*

Nicholas Lally
Lino Patti
Arthur Quaglieri
Robert T. Tierney

SUBSOILS OF BOSTON

Ronald C. Hirshfeld, *Chairman*

Richard F. Battles
Horst Borbereky
Donald T. Goldberg
James F. Haley
Rev. Daniel Linehan

AUDITING

Llewellyn T. Schofield
James P. Archibald

INVESTMENT

Paul A. Dunkerley, *Chairman*

Harl P. Aldrich, Jr.
Robert H. Culver

QUARTERS

Robert H. Culver, *Chairman*

Charles O. Baird, Jr.
Paul A. Dunkerley
Walter M. Newman
Herman G. Protze

B.S.C.E. - A.S.C.E. RELATIONS

Ernest L. Spencer, *Chairman*

James P. Archibald
William A. Henderson
Edward C. Keane
Robert J. Van Epps

BY-LAWS

Llewellyn T. Schofield, *Chairman*

George G. Bogren
Paul A. Dunkerley

NEWSLETTER EDITOR

Ronald E. Bucknam

JOHN R. FREEMAN FUND

Leslie J. Hooper, *Chairman*

David R. Campbell
Clyde W. Hubbard
George R. Rich
Lee Marc G. Wolman

RALPH W. HORNE FUND

William L. Hyland, *Chairman*

George G. Bogran
Miles N. Clair

FITZGERALD - HERSCHEL AWARD

Edwin B. Cobb, *Chairman*

Edward C. Keane
Saul Namyet

SANITARY SECTION AWARD

Joseph C. Lawler, *Chairman*

David A. Duncan
Robert L. Meserve

STRUCTURAL SECTION AWARD

John M. Biggs, *Chairman*

James F. Haley
Frank J. Heger
William L. Hyland
Charles C. Ladd

TRANSPORTATION SECTION AWARD

Edward C. Keane, *Chairman*

Alexander J. Bone
George C. Wey

HYDRAULICS SECTION AWARD

Arthur T. Ippen, *Chairman*

Allen J. Burdoin
Allen T. Gifford
Ronald T. McLaughlin
Lawrence C. Neale

CONSTRUCTION SECTION AWARD

Herman G. Protze, *Chairman*

Paul S. Crandall
William E. Wiley

NEW SECTIONS

Saul Namyet, *Chairman*

John M. Biggs
Donald T. Goldberg
Frank J. Heger
Charles C. Ladd
Frank K. Perkins
Gerald L. Woodland, Jr.